SIMPLE METEOR SCATTER OUT-STATION ANTENNAS

Ofer Givati

A dissertation submitted to the Faculty of Engineering, University of the Witwatersrand, Johannesburg, in fulfilment of the requirements for the degree of Master of Science in Engineering

Johannesburg, 1989

DECLARATION

I declare that this dissertation is my own, unaided work. It is being submitted for the Degree of Master of Science in Engineering in the University of the Witwatersrand, Johannesburg. It has not been submitted before for any degree or examination in any other University.

____
(Signature of candidate)

15th day of September 1989

ABSTRACT

This dissertation examines simple Meteor Burst Communication (MBC) out-station antennas. The effect of illumination gain, beamwidth and orientation was studied using computer simulation. Similarly, the performance of MBC links using a half-wave dipole, a quarter-wave monopole, a square loop, a long wire and a 5-elements Yagi-Uda antennas was determined. The performance of these links are related to the antennas' sky illumination. This investigation provides designers some bench-mark results which indicate the role played by the antennas' radiation patterns in MBC. A value system was formulated to provide practical and electrical trade-offs for mobile and manpack antennas in the meteor scatter environment. Simulated results indicate that simple antennas cause degraded communications due to their reduced size and complexity. The conclusion is that the directional master station should provide adequate sky illumination. It is recommended that the results obtained be validated by measurements and further work concentrate on master station antennas.

ACKNOWLEDGMENTS

I wish to acknowledge gratefully the following:

My wife Shelley and my sons Yaron and Yo'av for their support, love, consideration and encouragement at all times.

APC Fourie who always found the time to listen, support, guide and encourage when needed.

AR Clark for his helpful proof-reading.

Prof. HE Hanrahan for his kind guidance.

SALBU (PTY)Ltd. for their sponsorship.

CONTENTS

TABLE OF FIGURES

LIST OF SYMBOLS

Symbols	Description
λ	Is the wave length in meters.
λ_T	Is the transition wave-length defining the shortest wave-length for which equation (3) is applicable.
R_1 and R_2	Are respectively the points from transmitter and receiver to the point on the trail at which the reflection requirement is satisfied.
ϕ	Is half the angle between R_1 and R_2.
β	Is the angle between the trail axis and the plane containing the transmitter receiver and meteor trail at the centre of the principal Fresnel zone.
L	Half the length of the trail in the principal Fresnel zone.
Ψ_m	Defines a narrow band on the celestial sphere where meteor trails must lie in order to br properly oriented to produce a reflection between two stations.
L_T	Is the length of the meteor trail.
P_T	Is the transmitted power in Watts.
G_T and G_T	Are respectively, the transmitter and receiver antenna gain relative to an isotropic radiator immersed in free space.
r	Is the radius of the electron in meters.
q	Is the electron line density of the trail in electrons per metre.
q_m	Is the maximum electron line density in electrons per metre.
S	Is the dot product of a unit incident electric vector and a unit vector of the reflected wave in the direction of the polarization of the receiving antenna.

D	Is the ambipolar diffusion coefficient in m^2/sec.
r_0	Is the initial radius of the trail in meters.
τ and τ'	Are signal time constants.
t	Is the time measured from the formation of the trail in seconds.
μ_0	Is the permeability of free space.
e	Is the charge of an electron
m_e	Is the mass of an electron.
m	Is the initial mass of the meteor.
v	Is the meteor geocentric velocity.
v_H	Is the velocity of the meteor in its orbit around the sun.
v_E	Is the velocity of the earth *in its orbit around the sun.*
v_g	Is the geocentric velocity of meteors taking the earth's gravity into account.
ξ	Is the angle of the meteor radiant from the [illegible]
γ	Is the apparent angle of meteor radiant from th[illegible]s apex.
h	Is the meteor height in km.
h_{mi}	Is the height of maximum ionization.
H	Is the atmospheric scale height. This parameter depends on the temperature and degree of dissociation of the gas molecules at any given height.
μ	Is the angle between the incident electric vector on the trail and the electric vector at the receiving antenna.

α	Is the angle between the transmitter electric vector at the meteor trail and R_2
ζ	Is the zenith angle of meteor path axis.
B^1	Is the probability that a single atom will produce a free electron.
D_1	Is the antenna's directivity.
$U(\theta,\phi)_{max}$	Is the antenna's maximum radiation intensity.
U_{ave}	Is the antenna's radiation intensity averaged over all directions.
η	Is the radiation efficiency of the antenna.
T	Is the temperature in °K.
B	Is the bandwidth in Hz.
V	Is the rms value of noise voltage.
R	Is resistance in Ohms.
W_n	Is the noise power in Watts.

1 INTRODUCTION

1.1 Statement Of The Problem

Simple meteor scatter out-station antennas is the topic of this dissertation. The main thrust of this work is, therefore, two fold:

- To examine the effect of different illumination schemes of useful sky regions on Meteor Burst Communication (MBC) link performance.
- To evaluate the relative performance of MBC links using various standard simple out-station antennas. The performance of these are then related to the sky illumination they produce.

1.2 Introduction To Meteor Burst Communication

A *meteor particle is a solid body* that ordinarily revolves about the sun as part of our solar system. Each day billions of these meteors intersect the earth's orbit and penetrate its atmosphere. As the meteor enters the earth's atmosphere an ionized trail is formed which undergoes a rapid diffusion process and the density of the ionized particles in its trail permits the scattering of radio waves. Data transfer of an intermittent nature can thus be accomplished via these short lived trails provided their orientation obey some geometrical requirements. Hence the name: Meteor Burst Communication (MBC).

Commonly used methods for long range data telecommunications are telephone lines, radio repeaters stations, satellites and High Frequency (HF) communications using reflection from the ionosphere.

Telephone lines require a continuous interconnection between the nodes of a system. Radio repeaters stations require towers at line-of-sight distances between repeater sites, as well as power supplies. This presents an installation, maintenance and versatility problem. In recent years, satellites were thought to provide adequate coverage for long range communications. However, total dependency on satellites, due to their vulnerability to jamming and destruction, in addition to enormous capital outlay, has recently sparked the need to develop an alternative means of communication. Long range HF communications require large antennas and complex frequency management techniques due to changing ionospheric conditions [1,2,3].

MBC is a reliable alternative to these methods of long distance data communications for low volume applications. It offers a secure method for communications due to its jamming and intercept resistance characteristics. For any particular meteor trail there is a relatively small terrestrial "footprint" where the reflected signal is present, providing low probability of intercept (LPI) and jamming. This also ensures that a single frequency can be time-shared among many stations within a network, eliminating the need for multiple frequencies. In addition, MBC may also prove useful in maintaining post nuclear attack communications. Ionospheric disturbances associated with post nuclear attack conditions are expected to greatly increase D-layer absorption, which will in turn reduce the availability of HF communications [4,5,6].

The major drawback of MBC is due to the fact that only intermittent communication can be supported and hence voice communication, although possible, is still very limited [7]. However, latter-day computing power allows the use of short duration data communications signals. Such techniques have made MBC attractive for applications where intermittent communication can be tolerated. Undoubtedly, MBC systems present a scope for applications such as monitoring water levels in remote dams; safe, long distance communication for troops with their base station; the control of a fleet of trucks scattered over large distances as well as backing up existing communication methods.

1.3 Why Simple Antennas?

There exists a demand for meteor scatter communications in mobile, manpack and other situations where large and complex antennas are undesirable. This dissertation, therefore, examines aspects of simple out-station antennas for such applications. In this context, simple antennas are those complying with severe size and complexity constraints. Reducing the size and complexity of the antenna system inevitably results in communication systems of degraded connectivity and hence throughput. Connectivity, the fractional duration for which a channel exists, is a major aspect determining the quality of the link, while throughput is the amount of data transmitted per unit time. In the remote out-station MBC systems of interest, these aspects are traded off for simplicity.

1.4 The Investigation Of Simple Antennas For MBC

Before one can proceed to design simple antennas for MBC out-stations, it is imperative to understand the trade-offs involved with different sky illumination schemes. This outlines the importance of the role played by the antenna's radiation pattern which may be synthesized to achieve optimum performance. Having established these, one can study the relative performance of MBC links using traditional simple antennas. This provides important guide-lines for the antenna designer in terms of relative performance of various type of antennas in the meteor scatter environment. This work, therefore, is not intended to provide novel antenna designs but rather to evaluate traditional simple antennas and relate their performance to sky illumination. This will give designers some bench-mark results as well as an indication of the role played by the different illumination schemes.

Earlier research in this field was performed during the 1950's [8,9]. These studies illustrated the important role played by the antenna's radiation pattern in the medium of MBC. Of particular interest is the Hines et al. study of 1955 [8] examining the effect of:

(1) broadening the antenna beam centred on the transmitter receiver axis,

(2) swinging a narrow beam off to the side of the transmitter receiver axis, and

(3) swinging while broadening the beam, always maintaining its edge along the transmitter receiver axis.

However, even though Hines's study [8] may be of value in the design of antennas for MBC links it does not comprehensively outlines the effect of different illumination schemes of useful sky regions on MBC link performance. Nevertheless, it emphasised the need for a methodical and comprehensive investigation of this nature.

A prerequisite for a meaningful investigation of antennas is an understanding of the role of the antenna system played in MBC. Equally important are the mechanisms governing the behaviour of antennas. A review of this nature delineates the fundamental trade-offs concerned with physical constraints imposed by the remote antennas of interest, as well as these which are imposed by the medium. Once these trade-offs are established one may proceed to design suitable antennas.

The technique of value engineering hopes to quantify the trade-offs during design. The design phase of a product is a process whereby all the facts are organized to support a design concept which is later developed into a product. This process requires an organized synthesis of known factors and usually some creative thinking. There is often a single fundamental reason why new design is required. The technique of value engineering, resulting in a value system, is in essence an organized procedure for eliminating from a design all that is unnecessary. It ensures that the procedure has the opportunity of offering best overall value to the end user. Knowing what is required by the end user provides the guide-lines for the design. However, engineering design tools are also required to investigate different approaches for the development of the end product.

Powerful engineering tools were developed as a result of the availability of computing power. The availability of computing power which were not within reach until recent years led to the development of methods which allows rigorous simulation of antenna geometries and prompt the engineer towards solutions of such problems. Of particular use for the analysis of the electromagnetic response of antennas is the Method of Moments technique, which solves Maxwell's equations numerically for wire structures [10,11]. The problem of course in using this technique manifests itself in the loss of insight into the mechanisms of operation of the antennas and hence it should not be blindly used as a design tool but rather as the means to evaluate an antenna's performance.

A Method of Moment based software package is the NEC2 code [12]. Features include the facility to model wires and solid surfaces, the option of specifying many loads and sources, computation of radiation patterns and antenna interaction calculations. Another useful feature of the NEC2 code is that it allows modelling of imperfect earths and hence its effect on antenna performance can be investigated. The mathematical and numerical modelling of the antenna and its environment is the most important aspect of simulation where accurate results of performance are desired. Numerical limitations may be inherent either in the mathematical model used to approximate a physical system, the actual physical complexity of the system, or in the numerical techniques used for computation. The NEC2 code thus provide with the means to evaluate antennas.

The performance of an antenna, which is an integral part of an MBC link, cannot be viewed in isolation. The antenna's ultimate worth can only be established subject to its performance in the medium of MBC. A computer based predictive model which is designed to simulate a point-to-point MBC links is the METEOR code [13]. This engineering tool permits the setting up of an MBC link in terms of distance, time, orientation and antenna configuration, and computes the link performance in terms of meteor counts, antenna illumination, trail duration, noise and data communication.

The work reported in this dissertation uses these computer aided design tools for the simulation of antennas and MBC link performance. The technique of value engineering is applied to establish a value system for simple out-station antenna systems of interest.

1.5 Dissertation Layout

To conclude this introductory chapter a short preview of the remainder of this dissertation is outlined to emphasise its organisation.

The second chapter of this report commences with an overview of MBC and antenna theory. The nature of meteors and the geometry of an MBC link is delineated followed by a brief description of the mechanisms of reflection from underdense meteor trails. Next, a description of the computation method used to determine the number of meteor trails producing reflections arising from useful sky regions is out-lined to illustrate the importance of the role played by the antennas in the meteor scatter environment. Succeeding that, the merits of different types of antennas in the meteor scatter environment with emphasis on the antenna radiation pattern is presented. Thereafter, electrical problems due to antenna size limitation are outlined. The chapter concludes with a review of the effect of noise in relation to antennas. This chapter encapsulates the fundamental principles of MBC and emphasizes the role played by the antenna system.

The third chapter is devoted to design aspects of antennas for MBC. It presents a discussion on the technique of value engineering. This technique was used for the synthesis of a value system for the remote mobile and manpack MBC antenna systems. Thereafter the functional description of the Method of Moment based code, the NEC2 software package [12] is outlined with reference to numerical modelling constraints and limitations as imposed by the NEC2 code, deduced by experience gained in using the code, and structure modelling considerations. This is followed by, a brief description of the prediction software for MBC system performance, METEOR [13]. Finally, the relationships between antenna beamwidth/gain and orientation to waiting time between messages as well as channel duration are established. For this investigation, idealized radiation patterns were synthesized. These ideal patterns were utilized for different illumination schemes in order to establish the trade-offs in the meteor scatter environment.

The fourth chapter presents theoretical MBC link performance using simple antennas. Electrical performances of simple antennas were evaluated using the NEC2 [12]. The resulting radiation patterns were used to predict, with the prediction software METEOR [13], the effect of these simple antennas on MBC link throughput for stations separation ranging from 100km to 2000km. Both optimum antenna orientation as well as the worst case were considered.

The final chapter concludes this report with a short hindsight overview, *critical comments on* principle issues concerning simple meteor scatter out-station antennas as well as suggestions for further work.

2 BACKGROUND TO METEOR BURST COMMUNICATION AND THE ROLE PLAYED BY THE ANTENNA

In this chapter the process of radio waves scattering via meteor trails is briefly described outlining some important characteristics of MBC as well as its applications and limitations. Particular attention is paid to the peculiar geometrical requirements imposed by the MBC link, the mechanisms of reflection from underdense meteor trails and the variation in contribution of useful reflection from different sky regions. Once the importance of the role played by the antenna system becomes evident, the merits of different type of antennas in the medium of MBC are discussed. These include the antennas radiation pattern, electrical problems due to size limitation and the effect of noise on the antennas.

2.1 The Nature Of Meteors And MBC

Meteors form part of our solar system and travel in elliptical orbits with heliocentric velocities which are less than the solar escape velocity. The velocities of meteors approaching the earth range from 11.3km/s to 72km/s. The lower limit is the escape velocity of a particle leaving the earth. The upper limit is the sum of the escape velocity for a particle leaving the solar system (42km/s) and the earth's velocity around the sun (30km/s) [14,15]. Each day billions of meteors intercept the earth's atmosphere. It is estimated that on the average at least 10^{10} particles of mass greater than 10^{-5} grams are swept up by the earth daily [16]. Upon interception, the particle is heated by collision with air molecules, forming an ionized trail. The distribution of ionization along the trail is a function of the meteor mass, velocity, and angle of incidence [17]. These rapidly diffusing trails reflect radio signals, typically for hundreds of milliseconds during their brief existence, thus providing radio transmission paths over long distances. Typical spatial loss is in the order of 90dB in addition to about 80dB which is lost on scattering off a meteor trail. Therefore, MBC links are inherently weak signal systems [15,18,19].

Meteor trails occur in a region lying roughly between 80km and 120km above the earth's surface, called the meteor region, permitting MBC over distances up to approximately 2000km. The average length of a trail is 15km [17] while the diameter increases with time due to diffusion. This expansion causes rapidly weakening signal reflection and hence the duration for which it is useful for communication is limited. The reflected wave from a typical meteor trail illuminates a small area on the earth called the "footprint". This area of reception is estimated to be typically

8km wide by 40km long. The footprint, which is still being studied, appears to depend on the orientation, position and direction of travel of the meteors in space as well as the position of the receiver relative to the transmitter and the antenna pattern [2,17,20].

The communication link between transmitter and receiver is established only when these are properly oriented with respect to the meteor trail. This occurs when the angles of incidence and reflection on the trail are equal. Hence, the geometrical orientation results in a useful path when both the transmitter and receiver are located at the foci of an ellipsoid and the trail is tangential to the ellipsoid as illustrated in figure (1). This fixed-path geometry, coupled with the irregular arrival of meteors, causes a highly localized footprint. MBC, therefore, offers considerable advantages in terms of Low Probability of Intercept and high resistance to jamming [2,21].

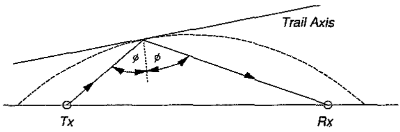

FIGURE 1: The geometry of the transmission path required for MBC.

The reflection of radio waves via meteor trails is a function of the ionization density distribution along and across the trail. In discussing the reflection properties it is customary to classify the trails either as "underdense" or "overdense". The dividing line, in terms of the electron density per metre of trail length, is $2x10^{14}$ electrons per metre which corresponds to the ionization produced by meteors of about 10^{-5} grams. Meteors trails with fewer than $2x10^{14}$ electrons per metre are referred to as underdense. Those with electron densities higher than this limit are termed overdense. Usable meteors for communication purposes typically have masses larger than 10^{-5} grams [15]. Smaller meteors will not produce sufficiently high electron density to reflect signals. The mass distribution of meteors is such that the total number of meteors greater than a certain mass is inversely proportional to that mass. The constant of proportionality is thus a measure of the influx rate and is dependent on time of day, year and the zenith angle with which meteors approach the upper atmosphere [18].

The low electron density of underdense trails allow the signal to penetrate through the ionized column, causing the signal to be scattered by the individual electrons. These electrons, which are excited by the radio wave, act as small dipole antennas and re-radiate the signal. The received signal energy is thus the vector sum of all discrete reflections. Since the diffusion of the trail is rapid, the phase difference increases and the amount of received energy reduces rapidly [2,15].

In overdense trails the electron density is sufficiently high to prevent complete penetration of the radio wave into the ionized column and therefore signals will be mostly reflected from the surface of the trails [15].

Due to the mass distribution of meteors, underdense trails are much more common than overdense ones and hence more useful as a medium for MBC. Overdense trails on the other hand produce high signal strength and longer usable duration for communication. From this it is clear that the MBC system design is based on the use of underdense trails while overdense trails enhance the link performances [6].

At certain times of the year meteor showers occur. These meteor showers are caused by a large number of particles moving with a common velocity about the sun and their orbit intersect the orbit of the earth at a specific times each year. They usually last for several hours only. This phenomenon only accounts for a small fraction of all meteors and is therefore of little use for reliable communications. Sporadic meteors which mostly follow random orbits about the sun and are incident upon the earth from all directions, play the most important role in MBC [14,15].

As pointed out before, the incident flux of sporadic meteors is a function of time of day, the season and the geographical location at the point of observation. The motion of the earth around the sun produces a diurnal variation in the rate of arrival of meteors, since the portion of the earth experiencing dawn (the apex in figure 2) will have the maximum surface area in the direction of the earth's movement. Thus, the apex will intercept many more meteors than the opposite side of the earth (the antiapex in figure 2) since only meteors of high velocity will overtake and intercept the earth [15,16]. Furthermore, the earth encounters a higher meteor density during the second half of the year, the period when it is closest to the sun. Some authors [6,21,22,23] believe that seasonal variations are due to the seasonal tilt of the northern hemisphere away from the earth's direction of travel. For this reasoning to hold true, the seasonal variations in the southern hemisphere would be the opposite of those experienced in the northern hemisphere. However, measurements taken in Adelaide [24], Australia, indicate similar annual trends to those in the northern hemisphere and the reason for this trend is therefore not clear.

The extent of diurnal variations in meteoric rate varies with latitude. An observer at the equator would encounter the greatest meteoric rate in the early morning hours since at that time the trajectory described by the earth about the sun is directly overhead. During the evening hours, only those meteors moving with velocities greater than that of the earth will be detected. An observer at the poles on the other hand would not observe any diurnal change in meteoric rate. To summarise: At moderate latitudes in either hemisphere the largest number of meteors will be entering the atmosphere at about 0600 local time and during the later half of the year. The smallest number will enter at about 1800 local time and in the first half of the year. The ratio of maximum to minimum depends on the latitude of the point of observation [16,24].

The diurnal and seasonal characteristics described above only considered the total meteor influx rate. The number of meteors available for useful communications depends not only on their influx rate, but also upon their radiants. The "radiant" is that point on the celestial sphere from which meteors appear to emanate. The radiant points are not uniformly distributed in the sky. They are, however, predominantly concentrated toward the ecliptic plane (the plane of the earth's orbit) and move in the same direction around the sun as the earth. The concentration of meteor radiants towards the apex of the earth's path, shown in figure (2), is the cardinal factor affecting the directional characteristics of a MBC link. This non-uniform distribution of meteors determine the relative importance of sky regions and hence the desired illumination pattern of an antenna for a particular link [25].

Not even all meteors intercepting the earth's atmosphere and which comply with the geometrical requirements of the MBC link are useful for communication. The usefulness of meteor echoes for communication depend upon their number as well as their individual duration. The duration that the signal remains above some predefined value, usually determined by the noise level, is called the duty cycle. The areas that contribute most to the duty cycle of an MBC link are those where the product of number and duration of meteors is a maximum and is most favourable for meteor propagation. These areas, as first shown by Eshleman and Manning [26], are located at either side of the midpoint between receiver and transmitter as illustrated in figure (3) and are referred to as "hot spots" [20,27]. However, the contour plot produced by Eshleman and Manning

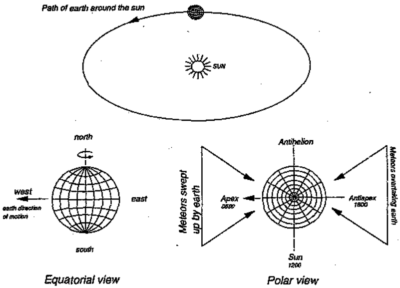

FIGURE 2: The earth orbit in the ecliptic plane illustrates the cause of diurnal variations of meteor rates.

[26] and later supported by Hines and Pugh [28] assumed uniform radiant distribution in calculating their results. Subsequent work illustrate [25], as stated before, non-isotropic meteor radiant distribution.

Clearly, the diurnal and seasonal variations in the radiant distribution on the celestial hemisphere above a particular meteor link control the relative magnitude and position of the two hot spots areas of meteor activity. Thus, as suggested by figure (3), the importance of one hot spot relative to the other may not be equal. Their shape and location varies diurnally, seasonally, with latitude and with path length as well as direction of communication path due to the non-uniform meteor radiant distribution [20,25]. Thus, these constantly changing hot spots characteristic is a significant factor in the design of antennas for MBC.

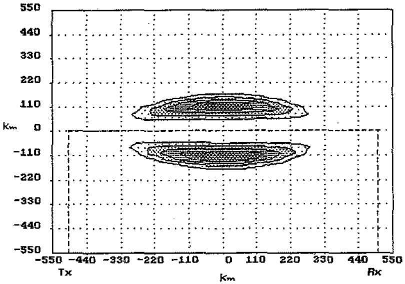

FIGURE 3: Plan view of the "hot spots" areas for MBC link over a north-south path of 1000km between terminals. These contours were computed by the prediction code METEOR [13]. Both transmitting and receiving antennas illuminate the sky with an idealized isotropic radiation pattern.

Another parameter effecting the quality of an MBC link is its operating frequency. The operating frequency of MBC systems may vary from 30MHz to 100MHz. Below 30MHz, the F-layer of the ionosphere may reflect the signal independently of the meteor trail as in normal High Frequency (HF) communication, giving rise to interference. On the other hand, power reflected from the meteor trails decreases with increasing frequency as will be shown in section 2.3. Above 50MHz the reflected power decreases rapidly with frequency and therefore a longer message waiting time as well as lower received signal strength will result. Hence, higher transmitter power would be required to achieve the same received signal strength. In general, frequencies ranging from 40MHz to 50MHz are preferred to minimize antenna size and allow practical levels of RF power [3].

Generally, MBC technology is ideally suited for applications such as telemetry and message based communication. A network would typically consist of a master station transceiver, which is a communication terminal with central processing controlling the system, one or more remote stations which could either comprise of communication or data terminals as illustrated in figure (4).

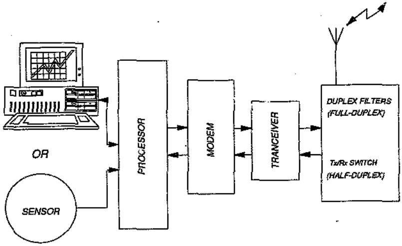

FIGURE 4: A typical configuration of a remote station.

2.2 The Geometry Of MBC Link

Since the majority of meteors used for communication exhibit underdense signal characteristics, the description of the scattering geometry will be restricted to this class of trails. The re-radiated fields can thus be used to estimate the amount of scatter [29].

The length of a meteor trail is primarily a function of the meteor mass and the zenith angle of approach into the upper atmosphere. The average length of a meteor trail is about 15km but the useful length of the trail for communication purposes is determined by the length of the principal Fresnel zone.

For a sufficient amount of energy to be reflected by the ionized trail, both the transmitter and receiver will be located at the foci of an ellipsoid to which the meteor trail is tangential as shown in figures (1) and (5). The total transmission path length between the terminals is a minimum for reflections from these tangent points, marking the centre of the principal Fresnel zone (point M in figure 5). The principal Fresnel zone is that region surrounding the tangent point where reflections between transmitter and receiver follow a path length of no more than a quarter wave length longer than the minimum path length. At the boundaries of this principal Fresnel zone, subsequent Fresnel zones are formed. Reflections from these further Fresnel zones will be in anti-phase to those from the previous Fresnel zones. Hence, the received signal energy may be thought of as coming from the principal Fresnel zone only, since more remote Fresnel zones, produce reflected fields which more or less cancel each other out [15,29,30].

Thus, the portion of the meteor trail confined to the principal Fresnel zone is, hence, only a small fraction of the trail length and need not be the region of the trail where the maximum ionization occurs. This geometry for a meteor burst propagation path is illustrated in figure (5).

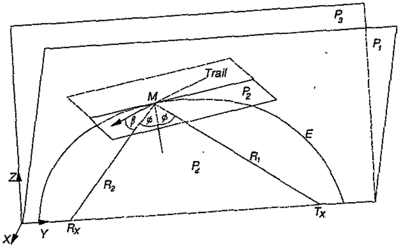

FIGURE 5: Scattering geometry.

In figure (5), P_4 is the plane of propagation defined by the transmitter, the scattering point M and the receiver. E is the ellipse defined by the intersection of the ellipsoid, with foci at the transmitter and receiver, and the plane P_1 of which P_4 is a sub-plane. The meteor trail is tangential to the ellipse E, and is contained in the tangential plane P_2 perpendicular to plane P_1. The centre of the principal Fresnel zone occurs where a meteor path is exactly tangential to E. The plane P_3 is a vertical plane from the transmitter to the receiver.

The total length of the trail in the principal Fresnel zone, 2L is given by:

$$L = \sqrt{\frac{\lambda R_1 R_2}{(R_1+R_2)(1-\sin^2\phi\cos^2\beta)}} \qquad (1)$$

Where:

- λ is the wave length in meters.
- R_1 and R_2 are respectively the points from transmitter and receiver to the point on the trail at which the reflection requirement is satisfied.
- ϕ is half the angle between R_1 and R_2.
- β is the angle between the trail axis and the plane containing the transmitter receiver and meteor trail at the centre of the principal Fresnel zone.

provided R_1 and R_2 are much greater than L.

Eshleman and Manning [18] stated that echoes will be received from points along a meteor trail other than those tangent to an ellipsoid defined by the foci at the receiver and transmitter. An echo will result when the angle, Ψ_m, between the tangent plane (P_2 of figure 5) and the meteor path satisfies:

$$\Psi_m \le \frac{L_T(R_1+R_2)}{4R_1R_2\cos\phi}(1-\sin^2\phi\cos^2\beta) \qquad (2)$$

Where L_T is the length of the meteor trail, and assuming that $L_T \ll R_1$ and R_2

2.3 Reflection From Underdense Meteor Trails

The distribution of energy reflected by a meteor trail is a function of many variables. A sample of these are the ionization density distribution along and across the trail, the signal frequency, the polarization of the incident wave relative to the antenna, the gain of the antennas and the motion of the trail with respect to the coordinate system.

As a result of the randomness of the various parameters, the *probability of two identical* reflections tends to zero. On the other hand, the complexity of the various mechanisms involved as well as the degree of uncertainty introduced leads to a situation where formulation of the physical problems are at best only useful approximations. They will apply rather well to some of the trails observed and quite poorly to others.

The derivation of transmission laws of reflections from underdense trails [15,31,32], are based on a mathematical model which assumes the trail to be a right-circular cylinder of electrons. *The diameter of these electrons is* much smaller than the signal wave length and their density within the trail is low enough for the incident wave to penetrate through the ionized column without major modification. This mathematical model is extended to account for the geometrical requirement that the trail be tangential to an ellipsoid with foci at the transmitter and receiver. Hence, the MBC link can "see" only a fraction of all trails incident on the ionosphere within its *range since* most do not have the proper orientation (outlined in section 2.2). For simplicity it is further assumed that the time taken for the meteor to traverse one half of the principal Fresnel zone is short compared with the duration, τ, required for the signal amplitude to decay to e^{-1} (the reciprocal of the natural logarithm base) of its initial value. That is, the time of formation of the meteor trail is assumed to be short compared with the total time that radio waves are scattered by the trail and hence transient effects are neglected. Thus, accounting for the length of the principal Fresnel zone, the received signal power scattered from an underdense trail can be estimated from the expression [15,31.32]:

$$P_R(t) = \frac{P_T G_T G_R \lambda^3 q^2 r^2 S^2}{16\pi^2 R_1 R_2 (R_1 + R_2)(1 - \sin^2\phi \cos^2\beta)} e^{-\left(\frac{r_0^2}{2D\tau}\right)} e^{-\left(2\frac{t}{\tau}\right)} \qquad (3)$$

Where:

P_T is the transmitted power in Watts.

G_T and G_T are respectively, the transmitter and receiver antenna gain relative to an isotropic radiator immersed in free space.

r is the radius of the *electron in meters.*

q is the electron line density of the trail in electrons per metre.

S is the dot product of a unit incident electric vector and a unit vector of the reflected wave in the direction of the polarization of the receiving antenna [32].

D is the ambipolar diffusion coefficient in m^2/sec.

r_0 *is the initial radius of the trail in meters.*

τ is the duration required for the signal amplitude to decay to e^{-1} of its initial value.

t is the time measured from the formation of the trail in seconds.

The *classical radius of the electron* is given by:

$$r = \frac{\mu_0 e^2}{4\pi m_e} = 2.8178 \times 10^{-15} \text{ metre} \tag{4}$$

Where μ_0 is the permeability of free space, e is the charge of the electron and m_e is the mass of *the electron.*

The time constant, τ, required for the signal amplitude to decay to e^{-1} of its initial value is given by:

$$\tau = \frac{\lambda^2 \sec^2 \phi}{16\pi^2 D} \tag{5}$$

In the derivation of equation (3) it was assumed, as pointed out before, that the formation time of a meteor trail is short compare with τ. However, the increase in the trail radius due to ambipolar diffusion during its formation can be appreciable. That is the ambipolar diffusion coefficient, D, may be large. Moreover, as indicated by equation (5), τ decreases as the square of the signal wave length. *Therefore, the above assumption does not* hold for short wave lengths, and/or large ambipolar diffusion coefficient.

The transition wave length, λ_T, is defined to be the shortest wave length for which equation (3) is applicable. This transition wave length may be estimated by equating the time of the formation of a meteor trail to the total time that radio waves are scattered by the trail. That is:

$$\frac{L}{v}=\frac{\lambda_T^2 \sec^2\phi}{16\pi^2 D} \qquad (6)$$

Where L is half the length of the principal Fresnel zone, given in equation (1), and v is the meteor velocity. Hence, combining equations (1) and (6), the transition wave length, λ_T, may be written as:

$$\lambda_T=\left[\left(\frac{16\pi^2 D}{v\sec^2\phi}\right)^2\left(\frac{R_1 R_2}{(R_1+R_2)(1-\sin^2\phi\cos^2\beta)}\right)\right]^{\frac{1}{5}} \qquad (7)$$

In practice, the parameters (such as D) upon which the transition wave length depend may vary in value. Therefore, it is necessary to evaluate the transition wave length for each specific case.

Diffusion commences as soon as a meteor trail is formed. Consequently, the radius of the trail increases with time and hence with distance from the meteor itself. To obtain the received signal from underdense trails, with wave length shorter than λ_T, the trail formation period should not be neglected. Accounting for this period, the received signal power is estimated as follows [15]:

$$P_R(t)=\left[\frac{P_T G_T G_R \lambda^6 q^2 r^2 \sec^4\phi\, S^2}{4096\pi^6 R_1^2 R_2^2 D^2}\right] e^{-\left(\frac{r_0^2}{2Dt}\right)}[1+K t^2]^{-1} \qquad (8)$$

Where:

$$K=\left(\frac{v^2\lambda\sec\phi(R_1+R_2)(1-\sin^2\phi\cos^2\beta)}{8\pi D R_1 R_2\cos\phi}\right)^2$$

Both equations, (3) and (8), illustrate how the transmission loss increases with signal frequency. While at frequencies below the transition frequency the transmission loss is proportional to λ^3, above that frequency the power falls as λ^6. The first factor in these equations represents the peak received power. The second factor accounts for the attenuation due to trail's initial radius. This loss arises due to interference between the re-radiation from the electrons within the trail whose thickness at formation is comparable with the signal wave length. The third factor indicates the received signal time dependence. This loss factor accounts for the increase in the trail radius due to ambipolar diffusion which can be significant even for as short a period as is required for the formation of the trail.

The variation of the received signal, at frequencies above the transition frequency, with time is as shown in figure (6).

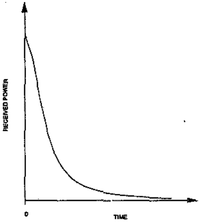

FIGURE 6: Time variation of the received power

Defining the duration, $\tau' = 1/\sqrt{K}$, of this signal as the duration of a rectangular pulse of equal energy with its peak value equal to the peak value of the received power [33], τ' may be expressed as follows:

$$\tau' = \left[\frac{8\pi^2 D R_1 R_2}{v^2 \lambda \sec^2\phi (R_1 + R_2)(1 - \sin^2\phi \cos^2\beta)} \right] \quad (9)$$

Comparing the expressions in equations (5) and (9) for the echo duration, it can be seen that at frequencies below the transition frequency τ *is proportional to* λ^2. *On the other hand*, at frequencies above the transition frequency, τ' is inversely proportional to λ. It may be argued that τ and τ' differ in their definition. Nevertheless, they both describe the usable echo duration and hence can be qualitatively unified. Quantitatively, τ is the time taken for the received power estimated in equation (3) to decay to about 0.37 of its initial value, while τ' is the duration taken for the received power in equation (5) to fall to about 0.29 of its peak value.

In order to obtain a practical estimate of the received signal power it is required to realistically approximate the various variable parameters on which it is dependent. A brief summary, delineating how some of these variables are quantified will be illustrative.

The velocity of a meteor approaching the earth is a function of the meteor's and the earth's orbital velocities around the sun and the angular distance of the radiant from the apex. This *geocentric velocity* of the meteor before coming under the influence of the earth's gravity may be expressed [31] as:

$$v^2 = v_H^2 + v_E^2 + 2\, v_H v_E \cos\xi \qquad (10)$$

Where v_H and v_E are respectively the velocity of the meteor and earth in their orbit around the sun and ξ is the angle of the radiant from the apex.

The geocentric velocity, v_g, taking the earth's gravity into account, may be written as [34]:

$$v_g^2 = 125 + v^2 \qquad (11)$$

The apparent angle of radiant from the apex, γ, for an observer on earth may be transformed as follows:

$$\gamma = \sin^{-1}\left(\frac{v_H}{v}\sin\xi\right) \qquad (12)$$

As mentioned before, the velocities of the meteors approaching the earth are in the range 11.3km/s to 72km/s. Clearly, equation (10) illustrates that meteors which emanate from angular distances, ξ, smaller than 90° are speeded up. Conversely, those meteors emanating from angles greater than 90° appear to be retarded. The correction introduced in equation (11) is based on Newton's law of gravitation.

As the meteor collides with air molecules, kinetic energy transforms to heat and the particle vaporizes. The velocity of the vaporized atoms is further restricted by air molecules, which ionize them by detachment. The ionization causes a trail of positive charged ions and free electrons, with an initial radius r_0, to form behind the meteor. The ionization left by the meteor is ordinarily in a shape of a cylindrical column which expands rapidly to a low density. The *ambipolar diffusion* coefficient, D, is a measure of how fast the trail diffuses and hence thins out. Both, the ambipolar diffusion coefficient and the initial radius are by no means constant and rather rapidly increase in magnitude with meteor height. This may be illustrated by an expression [35] which empirically relates the ambipolar diffusion coefficient to height in the region 80km to 110km as follow:

$$\log_{10} D = 0.067\,h - 5.6 \qquad (13)$$

Where D is in m^2/sec and h is in km. An empirical equation relating the initial radius to height [30] is as follows:

$$\log_{10} r_0 = 0.035\,h - 3.45 \qquad (14)$$

Where r_0 is the initial radius of the trail in meters.

Clearly, the characteristics and orientation of the antenna employed by the MBC link has direct bearing on the received signal power. It is, therefore, important to acquire a global overview of the various parameters governing the behaviour of this signal to gain insight of their *interdependences*. In the above transmission equation the factors of prime concern for the development of antennas are the polarization factor and the antenna gains.

The received signal power is directly proportional to $P_T G_T G_R q^2$. Thus, if transmitter power remain constant and the receiver threshold is unchanged then the minimum value of q can be reduced by increasing the gain of the antennas. Lower threshold value of electron line density, q, will in turn increase the number of detectable meteor trails illuminated and hence the link's duty cycle.

If both receiving and transmitting antennas are linearly polarized, the polarization factor, S, may be computed by defining the angle μ between the incident electric vector on the trail and the electric vector at the receiving antenna. Hence the polarization factor may be expressed as $S = \cos\mu$.

Alternatively, the angle between the incident electric vector and the direction of the scattering ray may be considered. That is, defining an angle α between the transmitter electric vector at the meteor trail and R_2, as shown in figure (7), will provide a measure of the change in polarization upon scattering. Maximum signal strength will be received when a *linearly polarized antenna* is oriented perpendicular to the plane of propagation since $\alpha = 90^{o}$ and $S = \sin\alpha$ will be unity [32].

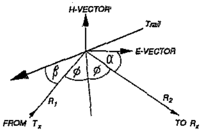

FIGURE 7: The transmitter electric vector at the meteor trail.

2.4 The Dependence Of Trails Detection On Sky Regions

The theoretical prediction of the relative contribution of sky regions to the detection of meteor trails commences by evaluation of the number of meteors whose electron line density exceed a minimum value as a function of meteor velocity, mass, zenith angle of trail axis and height above ground. It will be assumed [31, chapter 7] that all meteors have their point of maximum ionization at a mean height of 93km. Furthermore, it is assumed that the variation of electron line density with respect to maximum ionization at a given height is the same for all meteor trails. The maximum electron line density, q_m, in electrons per metre may be written as [36]:

$$q_m = k_1 B' m \cos\zeta \qquad (15)$$

Where:

- B' - is the probability that a single atom will produce a free electron.
- m - is the initial mass of the meteor.
- k_1 - is a constant of proportionality.
- ζ - is the zenith angle of meteor path axis.

M^{c}kinley [31, chapter 7] stated that $B' \propto v^5$, where v is the velocity of the meteor. Hence, on substitution into equation (15):

$$q_m = k_2 V^5 m \cos\zeta \tag{16}$$

Where k_2 is a constant of proportionality.

Following the above formulas presented by Kaiser [36], it was shown [17] that the number of free electrons produced per unit trail length, q, at atmospheric height h is given by:

$$\frac{q}{q_m} = \left(\frac{9}{4}\right) e^{\left(\frac{h_{mi}-h}{H}\right)} \left[1 - \left(\frac{1}{3}\right) e^{\left(\frac{h_{mi}-h}{H}\right)}\right]^2 \tag{17}$$

Where:

$h_{mi} = 93km$ - is the height of maximum ionization.

$H \approx 7km$ - is the atmospheric scale height. This parameter, as shown by Mckinley [31, chapter 7], depends on the temperature and degree of dissociation of the gas molecules at any given height.

Substituting equation (16) into equation (17) yields:

$$q = \left(\frac{9}{4}\right) m k_2 v^5 e^{\left(\frac{h_{mi}-h}{H}\right)} \left[1 - \left(\frac{1}{3}\right) e^{\left(\frac{h_{mi}-h}{H}\right)}\right]^2 \cos\zeta \tag{18}$$

The number of meteors of mass greater than m entering the earth's atmosphere per unit area per unit time given by [37]:

$$N(m) = \frac{k_3}{m^{k_4}} \tag{19}$$

$$k_3 = k_5 \cos\zeta \tag{20}$$

Where:

k_4 - is a constant. Based on experimental data [16], this constant has the value of about one.

k_5 - is a function of time of day and year also found empirically.

Combining equations (19) and (20) yields an expression for the number of meteors of mass greater than m entering the earth's atmosphere per unit area per second as follows:

$$N(m) = \frac{k_5 \cos\zeta}{m^{k_4}} \quad (21)$$

Substituting for the meteor mass in equation (21) from equation (18) results in the number of meteor trails with electron line density greater than q as follows:

$$N(q) = \left(\frac{k_2 v^5}{q\, f(h)}\right)^{k_4} k_5 \cos^{(k_4+1)}\zeta \quad (22)$$

Where:

$$f(h) = \left(\frac{4}{9}\right) e^{\left(\frac{h-h_{ml}}{H}\right)} \left[1 - \left(\frac{1}{3}\right) e^{\left(\frac{h_{ml}-h}{H}\right)}\right]^{-2}$$

Two different approaches were identified from the literature to approximate the rate at which usable underdense meteor trails are detected.

The first approach is based on the technique developed by Meeks and James [37] who assumed a uniform radiant distribution and maintained the geometric requirements for the establishment of an MBC channel. Prior to that, Pugh and Hines [28,38] have studied the uniform radiant distribution and refined the work earlier presented by Eshleman and Manning [26]. As pointed out in section 2.2, Eshleman and Manning [18] stated that echoes will be received when the angle, Ψ_m, between the tangent plane (P_2 of figure 5) and the meteor path satisfies equation (2).

The statement in equation (2) may be implemented by ignoring the requirement that meteors should traverse the plane in which a trail must lie within the principal Fresnel zone, and allowing them to lie in a band centred on that plane [18].

Hence, the number of meteor trails producing reflections, n(q), arising from a square kilometre of the plane at height h kilometres above the transmitter and receiver, representing the meteor trail zone, per second, may be computed by integrating N(q) over a band $2\Psi_m$. These bands are centred at the points of tangency of the meteor trail to the ellipsoid defined by the foci at the receiver and transmitter. Thus:

$$n(q) = \int\int_{band} N(q)\, dA \quad (23)$$

The second approach, is based on the work of Rudie [39] who improved on the work of Pugh *and Hines* [28,38] and Meeks and James [37] by accounting for some of their geometrical simplifications [40]. Rudie [39] developed a mathematical model for the radiant distribution, which approximates the empirical data reported by Davies [41]. However, it appears as though the major contribution of Rudie's work is in the development of the mathematics for coordinates transformation. He developed expressions to transform the distribution of meteor orbits from the heliocentric coordinate system to the distribution of meteor radiants. These radiants are the intersection of the meteor trails and the celestial sphere, observed on the earth. Computation of the number of detectable trails is performed for each point in the plane, at height h kilometres above the transmitter and receiver, which represents the meteor trail zone by integration with respect to height. At each height, between the lower and upper limits of the meteor region, only meteor trails which satisfy the requirement that meteors should traverse the plane in which a trail must lie to present a principal Fresnel zone are accounted for.

As shown, in this section and section 2.3, the observed occurrence rate of useful meteors and the mean received signal level is a function of the antenna system employed. The dependence can be predicted theoretically by combining the antenna illumination pattern with a model of meteor *trail distribution function, and then integrating* the product over the relevant volumetric sky region illuminated by the antennas.

2.5 The Merits Of Different Type Of Antennas In The Meteor Scatter Environment

The antenna is that component of the communication system which links and interfaces the transmitter and receiver networks to the medium through which signals propagate.

Owing to the small footprint, a single frequency may be time-shared among all stations within a meteor scatter network. Antenna bandwidth is, therefore, of little concern in MBC applications. *This simplifies the design, since broadband* antennas produce difficulties in term of pattern and impedance constancy. Manpack and mobile applications may necessitate the use of small antennas which are the main thrust of this research. Such antennas are inherently inefficient and this parameter will be considered in more detail.

Due to the concentration of useful meteors within the hot spots, it is clear that the antenna radiation pattern and its associated gain characteristics plays a predominant role in the meteor scatter environment. Since simple MBC systems operate at a fixed frequency, impedance matching is trivial and hence *considered to be of lesser importance.*

2.5.1 Antenna radiation pattern

The directional characteristics of an antenna is given by its radiation pattern. Whether operating in the transmitting or receiving mode, the pattern of the antenna is the same in accordance with the reciprocity theorem for antennas [42,43]. The antenna radiation pattern is a graphical representation of the relative strength of radiated fields as a function of the zenith, θ, and azimuth, ϕ, angles of the spherical coordinate system for a constant radial distance from the source. The radiation characteristics of an antenna is, therefore, represented by a three dimensional pattern.

Some important radiation characteristics are expressed in terms of scalar quantities. One useful measure of this is the directivity, D_i, which is the ratio of the maximum radiation intensity, $U(\theta,\phi)_{max}$ to the radiation intensity averaged over all directions, U_{ave}. The radiation intensity is a measure of the power radiated from an antenna per unit solid angle. Thus:

$$D_i(\theta,\phi) = \frac{U(\theta,\phi)_{max}}{U_{ave}} \qquad (24)$$

The gain of an antenna (referred to a lossless isotropic source) is a function of its directivity and efficiency. This efficiency accounts for ohmic losses arising from the conductivity of metal and dielectric losses. Thus, the gain of an antenna in a specified direction (θ,ϕ) is given by:

$$G(\theta,\phi) = \eta D_i(\theta,\phi) \qquad (25)$$

Where η is the radiation efficiency of the antenna. Although antenna's gain can be specified in any direction, it is usual to refer to the peak value which coincides with the direction of the main beam radiated by the antenna.

In the meteor scatter environment, the question to be addressed with regard to radiation pattern is whether better connectivity can be achieved by focusing a narrow beam onto a region where useful meteors are more likely. The radiation intensity in the main lobe of an antenna is, to a good approximation, inversely proportional to the angular width of the main lobe. As a corollary, the gain of the antenna is inversely proportional to the beamwidth in the zenith and azimuth planes.

The use of narrow beam antennas reduces the solid angle subtended and therefore the volume of sky illuminated. But the higher gain of the antenna compensates by increasing the observable number of meteors per solid angle. MBC simulation results [19] indicate that a split beam pattern directed at the hot spots to either sides of the transmitter receiver axis results in a larger number of useful meteor bursts per hour compare with a wide low-gain receiving beam directed at the transmitter.

2.5.2 Electrical problems due to size limitation

The requirements for radiation efficiency, as shown by the Chu-Harrington limit [44], indicate the trade off between efficiency, bandwidth and antenna size. The Chu-Harrington limits, obtained by assuming that all possible wave modes are excited in a sphere enclosing the radiating structure and its consequences, are illustrated in figures (8) [adapted from 44] and (9).

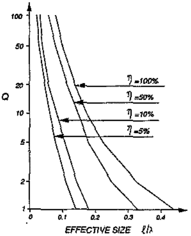

FIGURE 8: The chu-harrington limits.

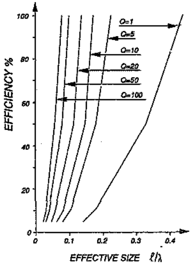

FIGURE 9: Consequences of the chu-harrington limits.

The effective Q-value of an antenna is a reciprocal measure of its bandwidth. These limits indicate that a reduction in the antenna's dimension would result in reduced efficiency for a fixed bandwidth. Furthermore, to achieve a desired efficiency performance while reducing the antenna's dimension would result in a higher effective Q-value (or reduction in the antenna's bandwidth). The antenna's bandwidth often suffers as a result of the reduction in dimension brought about to satisfy some practical constraints. This constraint is not a major problem in the simple meteor scatter environment, since such a system operate at a low data rate and hence requires narrow bandwidth. Directivity constraints due to size limitation is a more serious problem.

The directivity of an antenna with uniformly distributed electric field (ie. constant radiation pattern) across its aperture (termed aperture distribution) may be increased by large electric field fluctuations in the vicinity of the aperture's edges. This is known as superdirective condition [45, pp. 517-520]. Thus, antennas whose directivity is much larger than the directivity of a uniformly excited reference antenna of the same size is known as a superdirective antenna.

In an array, superdirectivity is achieved by insertion of multiple elements within a fixed length, thus decreasing the spacing. This causes large, out of phase currents to circulate within the elements, increasing the amount of recirculating energy, the effective Q of the array, and the ohmic loss, which in turn causes the antenna's efficiency to rapidly decrease. Superdirectivity, therefore, suffers from problems such as low radiation resistance and hence low efficiency, narrow tolerances due to large and oppositely directed currents and small bandwidth. Figure (10) [adapted from 44] is an example of such an array. It indicates the variation of Q with a directivity increase. A two wavelength long superdirective array, occupied by various numbers of isotropic elements illustrates an exponential increase of Q with directivity.

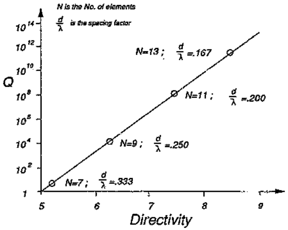

FIGURE 10: Q Vs Directivity computed for a 2λ array.

2.5.3 The effect of noise in relation to the antennas

The assessment of the effect of noise on MBC systems may be categorized in terms of internal and external interference. The internal source of noise is due to ohmic resistance of the antenna. External interference affecting the reception of VHF signals includes galactic noise, local atmospheric noise and man-made noise. The effect of noise on the MBC link is to decrease the usable signal duration since this is defined as the time period during which the signal-to-noise ratio is above a predefined limit. Hence, the system waiting time for transmission of an error free message frame is increased [46]. In the transmitting mode, the main requirement is to radiate as much of the available energy as possible, whereas in the receiving mode the main consideration is a good signal to noise ratio.

Owing to the thermal agitation of charges in a conductor, there is a certain amount of energy distributed over the whole radio frequency spectrum. The noise power (in Watts) resulting from this energy may be expressed as:

$$W_n = k\,T\,B = \frac{V^2}{4R} \qquad (26)$$

Where:

$k = 1.38 \times 10^{-23}$ J/°K is the Boltzmann's constant.

T is the temperature in °K.

B is the bandwidth in Hz.

V is the rms value of noise voltage.

R is the resistance in Ohms.

This level of noise power will always be present and is often used as reference.

Galactic noise, arriving from regions outside the earth's atmosphere, "seen" by an antenna depends both on its beamwidth and on the direction in which it is pointing. To minimize this effective noise temperature, the antenna beam should avoid pointing near discrete celestial radio sources. Although the presence of galactic noise appears to diminish as frequency is increased toward the GHz region, an isotropic noise temperature background will always prevail, independent of beam direction [47].

An atmospheric source of noise which may be significant at the VHF band is due to discharges taking place in the immediate vicinity of the receiving antenna. This form of noise, known as precipitation static, is caused by electrically charged particles which may be raindrops, snow, hailstones or dust clouds. Other sources of atmospheric noise is due to the currents caused by flashes of lightning. These currents are of such intensity and short duration that they produce a continuous spectrum of energy throughout the band of radio frequencies. Intermittent thunderstorm activity would give rise to impulse noise in a receiver, but the combined field of many flashes in a short time interval will appear as fluctuation noise [48].

Man-made noise include all noise sources due to electrical appliances and machinery. The lower portion of the VHF frequency spectrum is dominated by industrial equipment, with power lines and automobile ignition noise being major contributors [48].

Of all types of interference encountered, man-made noise is most severe [46,48]. Noise measurements, carried out by the Naval Ocean Systems Centre (NOSC) in the USA [46], indicate that man-made radio noise can be detected at distances in excess of hundred miles from large metropolitan centres and was found to increase with altitude. When man-made noise is eliminated by directing the antenna beam skywards, galactic noise predominates.

An indication of the expected noise levels in business, residential and rural areas is presented in figure (11). These correlations [49], however, should only be viewed as a yard stick since other factors, such as the orientation and height of the antenna above ground as well as the specific external interferences prevailing at a particular site at any point in time, will cause significant deviation from the indicated noise levels.

Figure (11) indicate median day-time values of surface man-made radio noise power and galactic noise power in dB above thermal noise, kTB, at 288°K as a function of frequency.

In general, noise sources should not be illuminated by the antenna's radiation pattern. Although noise cannot be completely eliminated, its level can be reduced. A significant reduction of man-made noise can be achieved by increasing the elevation angle of the main beam. In addition, minimising the height of the antenna above ground will reduce noise power int[illegible]uced via the antenna's minor lobes.

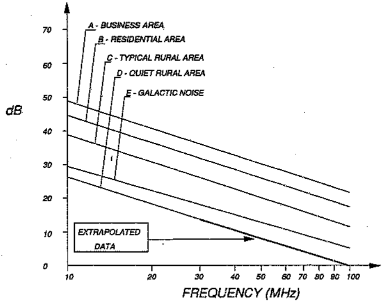

FIGURE 11: Average median day time values [49] of surface man-made radio noise power for a short vertical lossless grounded monopole antenna.

3 DESIGN OF SIMPLE ANTENNAS FOR MBC

In chapter 2 the a theoretical overview on the mechanisms of MBC and the role played by the antenna system was outlined. In this context the merits of different type of antennas in the meteor scatter environment are delineated. In this chapter design aspects of antennas for MBC are presented. These include the synthesis of value systems of antennas for mobile and manpack applications, a review of the design tools used to acquire theoretical results of MBC link performance using different antennas, and an examination of the merits of different sky illumination schemes for MBC.

3.1 A Value System For The Remote MBC Antenna System

Value may be defined as those qualities on which the worth, desirability or utility of the system depends. The objective of this remote MBC antenna value system aims at establishing antenna characteristics for design and evaluation to ensure the best overall antenna system for the end-user.

The value of a system is therefore perceived in terms of the degree to which it satisfies the end-user requirement. A value system is the result of value analysis, which is the analytical investigation of the factors or circumstances which affect the value of the system. Value analysis, is therefore, the process of weighing the various aspects of a system against each other in a quantitative fashion.

This procedure is a valuable tool during the normal design process. An engineer always aims at a good value, but is often concerned with the technical activities of the system and it is difficult for him to make an objective appraisal of the total system in its final application. The technique of value analysis provides a method whereby this could be methodically achieved.

The approach in value analysis is to identify the crucial aspects of the system and to assess these relative to each other. In the meteor scatter environment these functional virtues could typically be the size of the set, waiting time between messages, the size of the antenna, its ruggedness and the l... In the value analysis the user is forced to indicate the importance of the various functional aspects in comparison to all the others, thereby assigning a quantitative value to each. It is often discovered that a conventional design concentrates on areas of lesser importance and simultaneously high cost. These functional aspects of lesser importance are often the consequences of others which are in reality more important. If the designer is able to implement the design goal using alternative methods and thereby eliminate some, or all, of these less important aspects, a better system value is achieved.

The use of a value engineering technique requires considerable skill and judgment. One must guard against degrading the system at the expense of some quality which is not strictly functional, but which nevertheless contributes to its worth. This could include appearance, ultimate durability, transportability, maintainability and so forth. An attempt was made to formulate a value system for both mobile and manpack use in MBC. This attempt follows a procedure of value analysis suggested by GHW Bodman [50].

From the discussion on MBC and the role played by the antenna presented in chapter 2, it is clear that MBC require high gain antennas which are synthesized to illuminate specific sky regions. The type of illumination schemes best suited for MBC will be investigated in section 3.3. This will determine the shape of the antenna's radiation pattern ideally suited for optimum performance. But these desired characteristics may differ considerably to that which can be achieved using simple antennas due to complexity and size limitations. It may be found, for instance, that the ideal antenna should have horizontal beamwidth in the order of 8 degrees and vertical beamwidth, including ground effects, of about 6 degrees. Minor lobes should be about 40dB down on the main beam and the radiation efficiency of greater than 90 percent. The antenna should also illuminate the sky region at a height of about 95km above the mid-path between receiver and transmitter. Clearly, many of these idealized technical requirements clash with the requirement for a simple antenna, as it is difficult to obtain high directivity as well as accurate directionality of antennas mounted on moving vehicles. Hence, a value analysis indicates how the technical requirements can be optimally met while still satisfying the practical aspects of the system.

Mobile and manpack remote out-station antenna systems are of particular interest. In mobile MBC severe constraints are placed on the antenna, especially in terms of its height and ruggedness, whereas the size of the set itself is not of that much importance. The manpack remote station, on the other hand, may employ a more elaborate antenna, but the antenna must be collapsable and the weight of the set should be minimized. The size and weight of the set is related to its power capability. Clearly, remote out-station antennas of reduced size and complexity will result in communication systems of degraded throughput. Therefore, the waiting time between messages and their size will be traded off for simplicity. But just how important are these aspects in relation to one another? The answer to this must emerge from the value system analysis.

The procedure followed to determine the weighting of the various important aspects is such that a decision is forced to be made on a one-to-one basis. The relative importance of each aspect with respect to all other aspects is then determined. These can then be plotted to graphically illustrate groups of aspects with similar importance. Often, the groups with lower weighting are those which degrade the worth of the system. It may be possible to eliminate the less important aspects by different methods of implementing some of the more important ones, thereby enhancing the system's worth. Finally, any design of a system can be evaluated on the basis of how well the requirements, laid down by the value system, are fulfilled. The detailed procedure of value analysis used is outlined in Appendix A for the interested reader.

Following the procedure of value analysis presented in Appendix A, the value systems obtained for the remote mobile and manpack antenna systems in terms of priority and weighting are shown in figures (12) and (13) respectively. The weighting factors were arrived at after discussion between university researchers and engineers from SALBU(PTY)Ltd. [51] who were familiar with the end-user requirements.

MOBILE REMOTE OUT-STATION	
ASPECTS	*WEIGHTING*
Reduced height of antenna	*11*
Ruggedness of antenna	*9*
Short waiting time between messages	*7*
Reduced size of antenna	*4*
Large messages (Vs. short)	*4*
Limit No. of antennas to one only	*1*

FIGURE 12: The value systems for the mobile remote out-station antenna systems.

MANPACK REMOTE OUT-STATION	
ASPECTS	WEIGHTING
Small weight of set (power out)	10
Small size of collapsed antenna	9
Short waiting time between messages	9
Ruggedness of antenna	4
Ease of antenna orientation	2
Large messages (Vs. short)	1

FIGURE 13: The value systems for manpack remote [illegible]tation antenna systems.

Clearly, the weight of the set is of prime importance in the ma[illegible] station and is not important when mounted on vehicles. This finding has an ultimate bearing on the output power capability of these stations and consequently the implementation of the antenna system. Short waiting time between messages is an important functional aspect in both manpack and mobile applications while large messages are of considerably lesser importance, especially for manpack applications. The point of concern in the manpack situation is the problem of having to carry the equipment on one's back. As a result of this, the importance of having competent users to align and assemble the antenna system is evident. When an MBC link is mounted on a vehicle, it is the reduced height and ruggedness of the antenna which is important rather than its reduced size and complexity.

3.2 Computer Aided Analysis Of Antenna Performance And MBC Link Performance

The design of antennas must adhere to the value system establish for its specific application and thus examined in this light. But before this can be done, an evaluation of the performance of these antennas in terms of their electrical characteristics, as well as the performance of MBC links employing these antennas must be carried out. A powerful technique for the simulation of antennas is the Method of Moments described in Appendix B. In this work, The Method of Moment based code NEC2 [12] was used to evaluate antenna's performance. The performance of MBC links was theoretically predicted using the computer code METEOR [13].

3.2.1 Numerical Electromagnetic Code version 2, NEC2

The Numerical Electromagnetic Code version 2, NEC2, is a popular Method of Moments software package used for analysis of the electromagnetic response of antennas and other metal structures. The analysis is attained by the numerical solution of both an electric-field and magnetic-field integral equation for currents induced on the structure by sources or incident fields [12].

Results obtained by employing computer simulation of physical systems are only as reliable as their mathematical approximations, coupled with constraints imposed by numerical limitations. Numerical limitations may be inherent either in the mathematical model used to approximate a physical system, the actual physical complexity of a system, or in the numerical techniques used for computation.

The basic devices for modelling structures with the NEC2 code are short, straight segments for modelling wires, and flat patches for modelling surfaces. The proper choice of these segments and patches is critical in order to obtain accurate results. Some guide-lines appear in Appendix C as to the modelling technique and constraints to be followed when using NEC2.

The features of NEC2 include:

- Analysis of arbitrarily oriented wires and surfaces.
- Inclusion of a perfect ground plane, a real ground plane using Fresnel reflection coefficients or a real ground plane using the more rigorous Sommerfeld/Norton solutions.
- Up to 10 excitations can be specified on an antenna structure.
- Up to 30 lumped loads may be specified within the wire structure.
- The program output includes:
  - *Input impedance at the ports which were excited.*
  - Current distribution on the antenna.

- Both, near and far fields from the antenna.
- Efficiency of the antenna.
- Three dimensional radiation pattern.

In order to obtain valid results, the numerical and mathematical modelling of structures must obey a rigid set of rules imposed by the NEC2 code (see Appendix C). In addition, the input data file which interfaces the NEC2 code is row and column dependent. This constitutes a user unfriendly interface which demands a high level of expertise to use. Thus, an Intelligent Pre-processor for NEC2 was written [52]. The intent of this pre-processor is to keep the user isolated from the various constraints and limitations imposed by the NEC2 code as well as the automatic creation of the input data file.

3.2.2 Prediction software for MBC system performance

The computer code "METEOR" version 1.0 [13] is a prediction package for determining MBC link performance. This code is implemented as a utility for MBC designs in such a way that the user is permitted to set up the model of any point-to-point link in terms of its parameters. Three type of user modes are provided for:

- *The Novice mode: Permits the user to select* a predefined MBC link and instruct the computation of its performance.
- The User mode: For the more experienced user, allowing the setting of most of the important MBC link parameters.
- The Expert mode: Provides the user with complete control over the MBC system parameters, including the mathematical model used for computation.

This prediction tool allows the user to assess the data communication performance of an MBC link through the specification of the following parameters:

- Frequency.
- Transmit power.
- Receive sensitivity.
- Yagi-Uda antenna type and orientation or NEC2 input data file.
- Data rate and protocol specification.
- *Stations geographical location.*
- Local noise environment.

- Time of day and year.
- *Theory used for simulation.*

The output of the program include the prediction of:

- Relative contribution of various sky regions to detectable reflections.
- Antenna illumination contours and patterns.
- Absolute number of detectable meteors.
- Distribution of trails duration.
- Estimate of data communication performance.

Antenna illumination is computed by the program for Yagi-Uda antennas or using the NEC2 code. Using the NEC2 code allow for any radiation pattern to be incorporated in the computation of the MBC link performances. From the antenna designer view point, one of the useful aspects of the prediction model is its ability to predict MBC link performances for different antennas due to incorporation of NEC2 into this package.

The package enables the user to display measured results obtained for specific links during field tests. These results may be displayed together with the results computed by the prediction program. This facility serves to indicate the degree of confidence which may be placed on the ability of the package to produce accurate simulation results. In addition, it may be used to test the validity of different mathematical models employed for the computation of MBC link performances.

The prediction code METEOR [13] uses the two approaches outlined in section 2.4. In its computation of the number of detectable trails the underdense transmission equation of received signal power outlined in section 2.3 is employed. Furthermore, the contribution to the number of usable meteor trails in the plane h kilometres above the transmitter and receiver (used to represent the meteor trail zone) is calculated. This computation is carried out over the common sky region illuminated by the antennas.

3.3 The Effect Of Antenna Beamwidth/Directivity And Orientation On Meteor Burst Communication

In the preceding sections of this chapter the synthesis of value system for antennas was discussed *and the computer codes to predict antennas and MBC links performance were outlined. Since* meteor scatter propagation is dependent on antennas in a point-to-point link, base station as well as out station antennas need to be considered in this respect. This calls for an examination of the effect of different sky illumination schemes. In this section, therefore, the relationships between antenna beamwidth/gain to waiting time and channel duration are established.

3.3.1 Description Of The Experiment And Evaluation Method

The task of antennas employed by MBC systems is to illuminate sky regions where radio waves are most successfully reflected via meteor trails to establish channel openings. These regions of sky will, however, vary due to the migration of the hot spots discussed in section 2.1. Therefore, to examine the effect of different illumination schemes on the MBC link performance, a fixed link had to be considered at a set time. For the purpose of this study, an idealized radiation pattern was synthesized and used for illumination.

In this experiment, theoretical channel duration above threshold and meteor count results are presented for various idealized antenna illumination schemes over a 530km MBC link. These show that the correct choice of antenna directivity and orientation may dramatically enhance link performance. This investigation was repeated for a 1115km link to confirm the validity of the results.

The computer code METEOR [13] was used to predict the MBC link performance. As pointed out in section 3.2.2. some coefficient contained within the formulas implemented in this prediction model are adjustable. Hence, it is imperative to carefully calibrate the prediction model by comparison of results to empirical values before useful simulations can commence. The availability of measured data over 530km and 1115km paths was thus the reason for choosing these two representative links. The absolute numerical values resulting from simulation are therefore approximate, but the identified trends are reliable.

3.3.2 Test Link Description

The complete description of the MBC link and the various parametric settings of the prediction model used for this simulation are presented in Appendix D. An extract of the global features of this MBC link is as follows:

- *530km link.*

- Transmitter Latitude: 26° South
- Transmitter Longitude: 28° East
- Receiver Latitude: 30° South
- Receiver Longitude: 31° East
- 400W transceivers.
- 8kHz receiver bandwidth.
- 270°K receiver noise temperature.
- Minimum detectable signal strength of 10dB above noise.
- Trails with more than 60msec duration above threshold.
- A time of 06h00.

The antenna radiation pattern was synthesized to be a circular cone with uniform power *density over the cone solid angle and no illumination* elsewhere. For this idealized pattern there is a simple relationship between the cone angle, θ, and the isotropic directivity, D_i, approximated by:

$$D_i = 10\log_{10}\left(\frac{41253}{\theta^2}\right) \quad \text{dBi} \qquad (27)$$

The top view of the simulated link is shown in figure (14):

Three different types of transmitting/receiving antenna illumination schemes were investigated for this link

<u>Type 1:</u> Both receiver and transmitter beams are directed along the transmitter-receiver axis always illuminating the centre of the meteoric region (height 95km) at mid-path. The receiver beamwidth remains fixed at 72° as would be typical for mobile or manpack applications where simple antennas are used, while the transmitter beamwidth is incrementally reduced. The value of 72° was chosen to completely illuminate the hot spots regions.

<u>Type 2:</u> The receiver radiation pattern is the same as in Type 1. The transmitter illumination is centred on one hot spot only, while reducing its beamwidth and hence increasing directivity incrementally.

<u>Type 3:</u> Both receiver and transmitter are centred on one hot spot only, as the transmitter in Type 2, and the beamwidth of both are varied simultaneously.

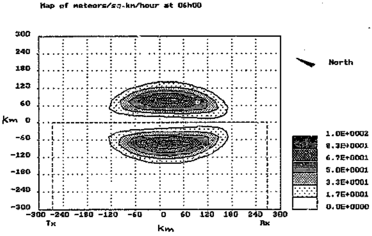

FIGURE 14: Contour chart of meteor distribution (computed by the prediction code METEOR [13]) for a 530km link with antennas radiating an idealized circular cone pattern of angle 72° directed at the link mid-point.

3.3.3 Results

Tabulated results are presented in Appendix E.

Figures (15) and (16) indicate optimum channel duration and rate of detectable underdense bursts at 13dBi (45° beamwidth) for type 1 illumination, 22dBi (16° beamwidth) for type 2 and 24dBi (12° beamwidth) for type 3. Figure (17) portrays the trade off between channel duration and useful meteors per hour seen for type 1 illumination. Similar trends are exhibited by illumination types 2 and 3.

Clearly, reducing the beamwidth and hence increasing the gain of the antennas beyond the optimum values, will result in degradation of the MBC link. To illustrate the importance of proper antenna choice and orientation, two practical cases are examined:

CASE A: Mobile and manpack antennas: A major improvement for this MBC application is possible by using an optimized master station antenna. To illustrate, using a Yagi-Uda antenna with gain of 13dBi (45° beamwidth) at the transmitting station and a 9dBi (72° beamwidth) antenna at the receiving station, as in Type 1, results in 110 meteors/hr as well

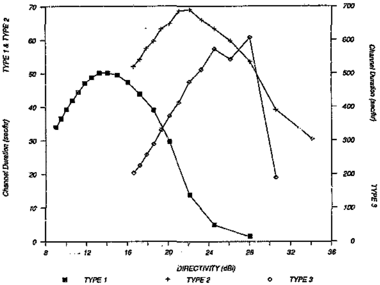

FIGURE 15: The graphs of Channel Duration Vs. Directivity for the three types of illuminations. Note: Scaling differences are indicated on vertical axes.

as 50 sec/hr channel duration. An optimized master station antenna with 21 dBi gain (18° beamwidth) and a 9dBi (72° beamwidth) remote station antenna, as in Type 2, yields 210 meteors/hr ; 70 sec/hr. A master station having two beams of the above optimum value was also simulated and produced an increase in the number of meteors/hr to 250 meteors/hr and the channel duration to 85 sec/hr.

Thus, to summarise, an optimum master station antenna for mobile communications will result in more than double the number of meteors/hr seen and approximately 70% increase of available channel duration.

CASE B: A fixed link MBC: Using the Yagi-Uda antennas with gain of 13dBi (45° beamwidth), directed along the Transmitter-Receiver axis, for both, master and remote stations results in 140 meteors/hr and 75 sec/hr. Using a 25dBi (12° beamwidth) antennas, directed at one hot spot only, as in Type 3, yields 1860 meteors/hr and 575 sec/hr. This is more than 10 times increase in the number of meteors seen per hour and over 7 times increase

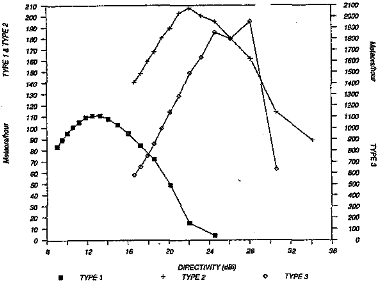

FIGURE 16: The graphs of useful Meteors per hour Vs. Directivity for the three types of illuminations. Note: Scaling differences are indicated on vertical axes.

in available channel duration. It is possible that these theoretical results are numerically somewhat higher than those which can be achieved in practice. Nevertheless, the trend is believed to be correct. A master station having two beams of this optimum value each, directed at the different hot spots, was also simulated and produced an increase in the number of meteors seen and channel duration by approximately 23%.

From this investigation it is clear that proper antenna choice and orientation particularly at the master station (for mobile communications) will result in dramatic link improvement. It should be noted that such optimum antennas are not unrealistic since a stacked array of 8 Yagi-Uda antennas with 5 elements each produce about 21dBi gain. For networking applications, however, steerable arrays will provide a more versatile solution.

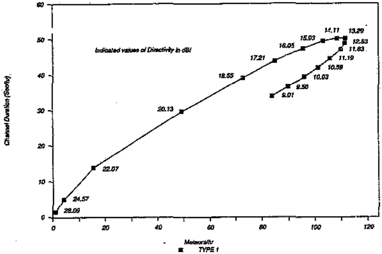

FIGURE 17: The graphs of Channel Duration Vs. useful Meteors per hour for type 1 illumination (shown in figures (15) and (16)). Directivity of illumination is indicated.

4 PREDICTION OF MBC LINK PERFORMANCE USING SIMPLE ANTENNAS

The study outlined in section 3.3 illustrated the importance of the correct choice of antenna directivity, radiation pattern and orientation in the meteor scatter environment. The requirement for simple antenna systems for mobile and manpack applications results in communication systems of degraded throughput. As indicated by the value system analysis (in section 3.1) for the mobile out-station, a higher weighting of importance is placed on the antenna's height and ruggedness than on the demand for short waiting time between messages. For the manpack remote station, the small weight of the set as well as the small size and collapsability of the antenna, out-weighs the requirement for short waiting time between massages. In view of this gride-line information one can now examine the performance of MBC links employing different antennas.

In this chapter, theoretical channel duration above threshold and meteor count results are presented, using various simple antennas, for stations separation ranging from 100km to 2000km. Tabulated results are presented in Appendix E.

4.1 Description Of Evaluation Method

The objective of this investigation is to establish performance of MBC links employing simple antennas. The performance of these, however, can only be useful if viewed on a reference basis. That is, the performance predicted for links employing any specific antènna should be viewed with respect to these same links employing other antennas. As reference antennas, therefore, a dipole antenna and its monopole ve sion were studied. Another useful reference antenna is a 5-elements Yagi-Uda antenna since this is often used for MBC. Subsequent simulations were performed for a mobile square loop antenna and a manpack long wire (terminated) antenna. The antennas were deliberately simulated either in free space or above an infinite conducting ground in order to eliminate the varying effect of real ground on the antenna's radiation pattern. Clearly, in practical cases the *NEC2* code may be used to determine the radiation pattern due to a particular ground plane. These theoretical results are presented for:

- 400W transceivers.
- 8kHz receiver bandwidth.
- 270°K receiver noise temperature.
- Minimum detectable signal strength of 10dB above noise.

- Trails with more than 60msec duration above threshold.
- A time of 06h00.

The transmitting station of the MBC link, fixed at longitude 28° east and latitude 26° south, employs a 5 elements Yagi-Uda antenna with radiation pattern as shown in figures (18) and (19).

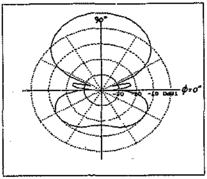

FIGURE 18: The azimuth-plane radiation pattern of the 5 elements Yagi-Uda mounted at the transmitting station. Maximum forward gain: 10.1dBi as evaluated by NEC2 [12].

This transmitting antenna is directed along the transmitter-receiver axis always illuminating the centre of the meteoric region (height 95km) at mid-path. The receiving station is not fixed. It traverses a north-south path along longitude 28° east, varying its latitude location from 100km to 2000km south of the transmitting station. All other settings of the prediction model used [13] are identical to those used in section 3.3. These can be viewed in Appendix D.

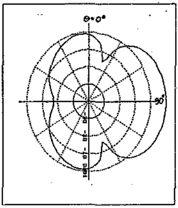

FIGURE 19: The elevation-plane radiation pattern of the 5 elements Yagi-Uda mounted at the transmitting station. Maximum forward gain: 10.1dBi as evaluated by NEC2 [12].

4.2 Evaluation Of Traditional Simple Antennas

The simplest antenna is possibly the traditional dipole. In accordance with the theory of images [53], a dipole antenna of arbitrary length can be modelled by mounting a monopole of half that length orthogonal to an infinite perfectly conducting ground plane. This monopole must then be fed at the ground point. The input impedance of a monopole is half that of a twice longer dipole but their radiation patterns are identical in the hemisphere above the ground. The gain of the monopole arrangement, however, is 3dBi above that of the dipole in free space, due to the presence of ground.

Since simple antennas are investigated, it is prudent to present the communications performance that one may expect using traditional simple antennas in the meteor scatter environment. For this purpose, performances of the horizontally polarized half-wave dipole in free space as well as the vertically polarized and a 45° skew quarter-wave monopole above an infinite conducting ground are studied.

4.2.1 adiation patterns of the traditional simple antennas

The radiation patterns of the horizontally polarizes half-wave dipole, the vertically polarized quarter-wave monopole and the 45° skew quarter-wave monopole are evaluated by NEC2 [12]. These are presented in figures (20), (21), (23) and (24). The orientation of the skew quarter-wave monopole in the spherical coordinate system is such that its structure's zenith angle $\theta = 45°$ and azimuth angle $\phi = 90°$ as shown in figure (22).

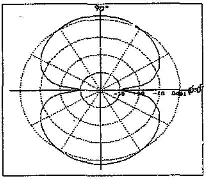

FIGURE 20: The azimuth-plane radiation pattern of the half-wave dipole antenna in free space. Maximum forward gain: 2.16dBi. The elevation-plane pattern is omitted since it is constant in the ZY-plane for a dipole in free space oriented along the X-axis.

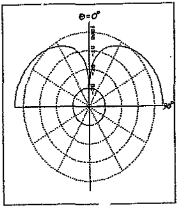

FIGURE 21: The elevation-plane radiation pattern of the quarter-wave monopole antenna on a perfectly conducting infinite ground plane. Maximum forward gain: 5.16dBi. The azimuth-plane pattern is omitted since it is constant.

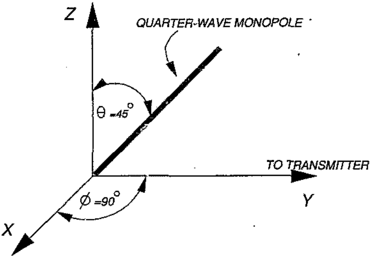

FIGURE 22: The orientation of the skew quarter-wave monopole.

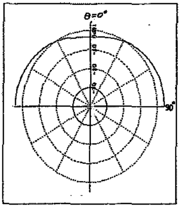

FIGURE 23: The elevation-plane radiation pattern of a 45° skew quarter-wave monopole antenna on a perfectly conducting infinite ground plane (from azimuth view-point $\phi = 90°$). Maximum forward gain: 4.65dBi.

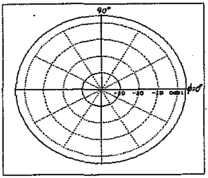

FIGURE 24: The azimuth-plane radiation pattern of a 45° skew quarter-wave *monopole antenna on* a perfectly conducting infinite ground plane. Maximum forward gain: 4.65dBi.

The maximum forward gain of the skew monopole occurs at $\theta = 90°$ while $\phi = 0°$ and $\phi = 180°$ respectively. At $\phi = 90°$ and $\phi = 270°$ the gain drops by about 0.3dB. This marginal drop in gain cannot be easily seen in figure (24).

4.2.2 Results predicted by METEOR for the traditional simple antennas

Figures (25) and (26) indicate that the optimum orientation of the half-wave dipole is at right angle to the transmitter-receiver axis while that of the quarter-wave monopole is at vertical position. The optimum orientation of the skew quarter-wave monopole in the azimuth-plane is at right angle to the transmitter-receiver axis while its worst orientation is along that axis.

For channel duration, as seen in figure (25), the optimum stations separation for the half-wave dipole is about 1000km. Both, the channel duration and the optimum stations separation decreases as this antenna is rotated through 90° in the azimuth-plane. The optimum distance between stations for the quarter-wave monopole is about 600km and channel duration is decreased as the zenith angle by which this antenna is skewed increases.

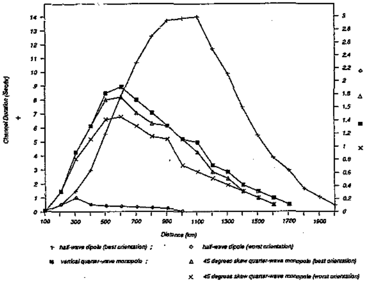

FIGURE 25: The graphs of Channel Duration Vs. Distance for the half-wave dipole and quarter-wave monopole at various orientations. Note: Scaling differences are indicated by symbols on vertical axes.

For average waiting time between useful meteors, which is inversely proportional to the meteoric rate, as shown in figure (26), the optimum station separation for the half-wave dipole is about 800km. Both, the number of useful meteors seen per hour and optimum distance between stations decreases as the dipole is rotated through 90° in the azimuth-plane. The optimum station separation for the quarter-wave monopole is about 500km and the meteor count is decreased as the zenith angle by which the monopole is skewed increases.

The half-wave dipole provide improved connectivity compare to that which is achieved employing the quarter-wave monopole. Figures (20) and (21) indicate that greater sky regions are illuminated by the dipole antenna, particularly at short range. As the distance between stations increases, the higher gain illumination of the monopole covers increasingly greater regions of sky and would, therefore, be expected to perform better than indicated in figures

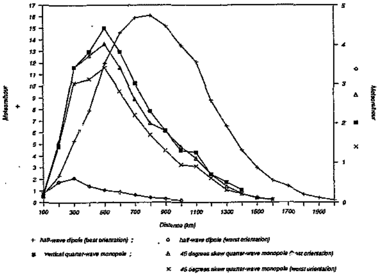

FIGURE 26: The graphs of useful Meteors per hour Vs. Distance for the half-wave dipole and quarter-wave monopole at various orientations. Note: Scaling differences are indicated by symbols on vertical axes.

(25) and (26). However, apart for overall degraded connectivity, the optimum station separation for the monopole antenna is shorter than that which is indicated for the dipole antenna.

Nes [54] reports that a vertically polarized wave would suffer a 3-4dB larger loss than a horizontally polarized one. The aim of this work, however, is not to qualify this statement but rather to examine the overall effect of different illumination patterns using simple antennas. Nevertheless, this may explain the superiority of the dipole antenna over the monopole for MBC. From a practical view-point, on the other hand, the orientation of the dipole antenna is very critical in order to achieve optimum performance, while that of the monopole is not critical at all.

4.3 Evaluation Of A Mobile Square Loop Antenna

For mobile applications, the vertically polarized quarter-wave monopole described above is deemed to be a suitable antenna configuration. Many different types of simple antenna configurations may be designed for mobile applications. However, in order to investigate the effect of different illumination patterns of antennas, a horizontally polarized square loop antenna (shown in figure 27) of a quarter-wave long sides was simulated. This square loop antenna complies with the requirements for ruggedness and reduced height. Moreover, its size would not exceed the roof area of an ordinary truck cabin.

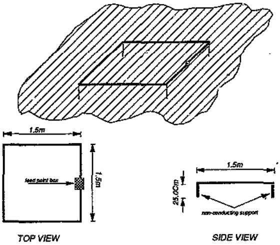

FIGURE 27: A mobile square loop antenna.

4.3.1 Radiation patterns of the square loop antenna

This square loop antenna when placed at a height of 0.25m above and parallel to an infinite conducting ground plane, has radiation pattern as shown in figures (28) and (29).

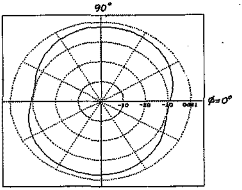

FIGURE 28: The azimuth-plane radiation pattern of the square loop antenna *sliced at zenith angle $\theta = 70°$ as computed by NEC2 [12].*

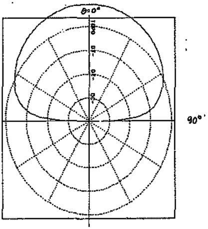

FIGURE 29: The elevation-plane radiation pattern of the square loop antenna. Maximum upward gain: 9.5dBi as evaluated by NEC2 [12].

As seen in figure (29), a square loop antenna which is place parallel at a small height above a metal truck roof will radiate mostly upwards. The azimuth-plane radiation pattern, shown in figure (28), is nearly omnidirectional but the direction of the pattern maximum is seen tilted by about 12° from the Y-axis (azimuth angle $\phi = 90°$). This radiation pattern resulted from the dimension of the loop (a wavelength circumference) as well as its proximity to the ground plane. But since the roof is of finite dimensions and in practice will be only slightly larger than the area occupied by the loop antenna, the radiation pattern of such an antenna will actually be directed to the sides (zenith angle $\theta > \pm 90^{\circ}$) as well. As a consequence of this, the upward gain of the loop antenna will be somewhat reduced. This effect is favourable for MBC, as may be deduced from the performance of the half-wave dipole shown in figures (25) and (26), since greater volume of useful sky will be illuminated. On the other hand, directing the main beam vertically upward while reducing its height above the ground plane is desirable in order to reduce the effect of man-made noise (discussed in section 2.5.3). However, as outlined in section 2.5.2, decreasing the spacing between the loop antenna and the ground plane causes a rapid decrease of the structure's input impedance. The antenna's input impedance needs to be matched when coupled to the MBC link. Thus, the height of the loop above the ground was established to allow a practical impedance transformation ratio.

4.3.2 Results predicted by METEOR for the square loop antenna

The performance of this horizontally polarized square loop antenna in the meteor scatter environment, compared with that of the quarter-wave monopole described above, can be viewed in figures (30) and (31).

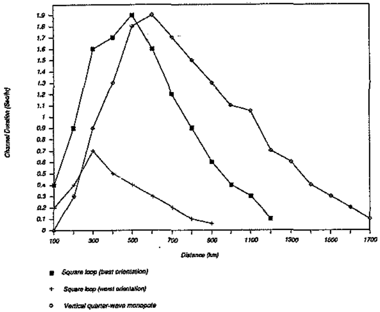

FIGURE 30: The graphs of Channel Duration Vs. Distance for the square loop and the quarter-wave monopole antennas.

Figures (30) and (31) shows that while the square loop antenna will provide better connectivity at short ranges (up to 500km), provided its orientation is optimal, the vertical quarter-wave monopole on an infinite conducting ground plane will enhance communications at ranges exceeding 500km. Nevertheless, it should again be noted that in practice, this ground plane is finite and hence will produce slightly different performance to that indicated.

From figures (21) and (29) it is clear that the quarter-wave monopole [illegible] a low take-off angle while the square loop is directed vertically upwards from the receiving antenna. The superiority of the loop antenna over the quarter-wave monopole at short ranges can be explained by noting that it illuminates a larger portion of the hot spots. As the stations separation increases, the quarter-wave monopole illuminate a greater portion of the important *sky regions and hence provide better connectivity.*

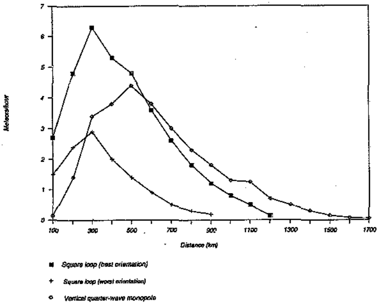

FIGURE 31: The graphs of useful Meteors per hour Vs. Distance for the square loop and the quarter-wave monopole antennas.

Since the radiation pattern of this square loop antenna is directed mainly at sky regions above the receiving station, the effect of illuminating these sky regions by the transmitting antenna with higher gain was examined. For this purpose, the transmitting 5 elements Yagi-Uda antenna which thus far was directed at the link mid-point (height 95km) was aimed at the link end-point (height 95km above the receiving square loop antenna). The results, as shown in figures (32) and (33), indicate that these two types of illumination schemes produce almost identical results. It can therefore be concluded that there is no advantage in illuminating the end-path when using these antenna. The idea of end-path illumination using different antennas should, however, be further investigated.

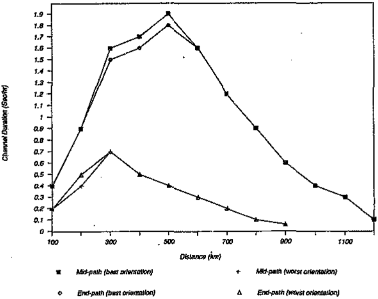

FIGURE 32: The graphs of Channel Duration Vs. Distance for the square loop antenna with the transmitting Yagi-Uda antenna *illuminating* the *mid-point* and end-point of the link.

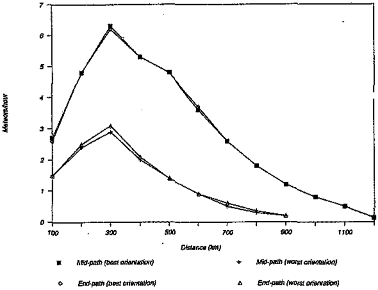

FIGURE 33: The graphs of useful Meteors per hour Vs. Distance for the square loop antenna with the transmitting Yagi-Uda antenna illuminating the mid-point and end-point of the link.

4.4 Evaluation Of A Manpack Long Linear Terminated Wire Antenna

The value system developed in section 3.1 indicates that the most important features of a manpack remote out-station are the small weight of the set, the small size of the collapsed antenna and short waiting time between messages. In section 3.3, the importance of illuminating the hot-spots with sufficient intensity was established. The main beam take-off angle of a long linear wire antenna can be adjusted by varying its length. Generally, the longer wire produces a smaller main beam take-off angle. This feature may be used for partial illumination of the hot spots located at either sides of the transmitter-receiver axis. In addition, this lightweight antenna can be realized using a thin flex wire which may rolled into a small bundle. These features make it attractive for manpack applications. Thus, a 146.5m long linear antenna (shown in figure 34), terminated by a 200Ω resistive load, was simulated. Altshuler [55], who carried out pioneering work on resistively loaded wire antennas showed that the insertion of a suitable resistance one quarter of a wavelength from the end of the monopole effectively terminates the antenna geometry by its characteristic impedance. Hence a travelling wave current distribution is produced between the source and the termination.

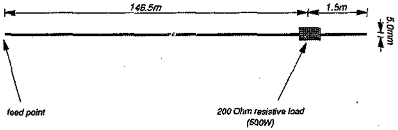

FIGURE 34: A long linear terminated wire antenna.

4.4.1 Radiation pattern of the long linear terminated wire antenna

The length of this antenna was chosen to be 146.5m so it can radiate with a narrow beamwidth and high gain at about 10° to the sides of the transmitter-receiver axis, enabling partial illumination of the hot spots. At short ranges the antenna was tilted to higher take-off angles for optimum illumination. The long wire antenna shown in figure (34), when placed at a height of 2m above and parallel to an infinite conducting ground plane, has radiation pattern as indicated in figures (35) and (36).

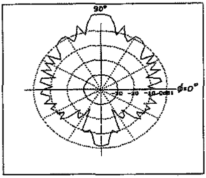

FIGURE 35: The azimuth-plane radiation pattern of the long linear (terminated) antenna *sliced at zenith angle $\theta = 80°$ as computed by* NEC2 *[12].*

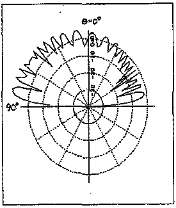

FIGURE 36: The elevation-plane radiation pattern of the long linear (terminated) antenna. Maximum forward gain: 12dBi as evaluated by NEC2 [12].

Radiation patterns will not be presented for the various tilt angles, but are similar to the one shown above with somewhat increased gain. The correct orientation of this travelling wave antenna can be achieved by the use of a balloon and ropes to control its elevation angle and direction.

4.4.2 Results predicted by METEOR for the long terminated wire antenna

The performances of this long wire antenna is compared with the 5 elements Yagi-Uda antenna (pointed to mid-path) and the half-wave dipole described before. These results are presented in figures (37) and (38).

For channel duration, the optimum stations separation is about 1000km for the long wire antenna and about 1300km for the Yagi-Uda antenna. For meteor count (or average waiting time), the optimum range is about 1000km for the long wire antenna, and about 1100km for the Yagi-Uda antenna. Optimum illumination of the hot spots is difficult to achieve with the long wire antenna due to ground effects and multiple nulls. Therefore, the curves presenting the results for the long wire antenna are not smooth.

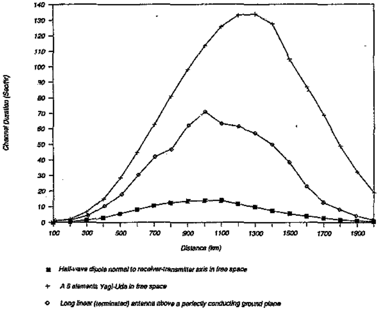

FIGURE 37: The graphs of Channel Duration Vs. Distance for the long (terminated) wire, 5 elements Yagi-Uda and half-wave dipole antennas.

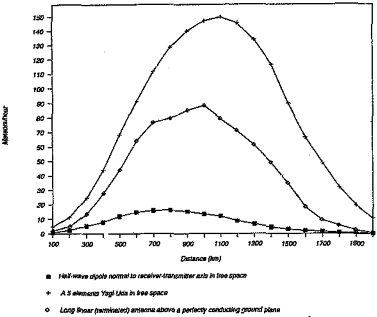

FIGURE 38: The graphs of useful Meteors per hour Vs. Distance for the long (terminated) wire, 5 elements Yagi-Uda and half-wave dipole antennas.

These results clearly indicate the importance of the antenna's gain and illumination pattern. The Yagi-Uda and the long wire antennas have maximum forward gains of comparable magnitude. The main beam produced by the Yagi-Uda antenna, however, is much wider than that produced by the long wire antenna. Hence, larger portion of useful sky regions can be illuminated by the Yagi-Uda antenna which results in improved connectivity. On the other hand, the half-wave dipole antenna's beamwidth is comparable to that produced by the Yagi-Uda antenna, but with much reduced gain. Thus using the dipole antenna results in poorer connectivity than can be achieved when using the Yagi-Uda and the long wire antennas.

4.5 Summary Of Results

The take-off angle required for mid-path illumination at 100km station separation is about 59°. This angle decreases as the distance between stations increases. The elevation-plane radiation pattern of the half-wave dipole in free space is constant in the ZY-plane (see figure (20)). Similarly, the azimuth-plane radiation pattern of the vertical monopole is constant at any elevation angle (see figure (21)). Thus, as seen in figures (20) and (21), at short ranges the half-wave dipole antenna provides better illumination of useful sky regions than the quarter-wave monopole antenna. As the station separation increases, the illumination pattern produced by the monopole antenna will cover a greater portion of useful sky regions with improved gain. In fact, using the illumination pattern and gain argument, at large distances the monopole antenna would be expected to provide with improved connectivity to that which may be achieved with the dipole antenna. However, theoretical results (presented in figures (25) and (26)) indicate that the half-wave dipole provide with better connectivity at all distances. This may be explained by the effect of antenna polarization on MBC performance. As discussed in section 2.3 and pointed out in section 4.2.2, a horizontally polarized antenna performs better than a vertically polarized antenna in the meteor scatter environment.

The half-wave dipole antenna, modelled in free space, was included in this investigation as a *reference antenna*. The square loop and the monopole antennas were considered to be suitable for mobile applications. The radiation pattern produced by the square loop antenna is directed vertically upwards, with high gain, to illuminate mainly sky regions above the receiving station (as shown in figure (29)). At short ranges (up to 300km) this loop antenna performs better than the half-wave dipole (as can be seen when comparing figures (30) and (31) to (25) and (26)). As the station separation increases, the connectivity achieved with the square loop antenna is rapidly degraded below that which may be achieved using a quarter-wave monopole. This is due to the fact that it illuminates smaller portions of useful sky regions as the station separation increases. However, as pointed out before, in practice this loop antenna will be place above a finite conducting plane. As a consequence, it is expected to illuminate a larger volume of sky at the expense of reduced upward gain and thereby offer improved connectivity.

As shown in figures (37) and (38), much improved connectivity can be achieved with a long wire manpack antenna compare to that which can be realized using mobile antennas. This is due to the requirements differences in the value systems (discussed in section 3.1) established for the remote mobile and manpack antenna systems in terms of priority and weighting. While *for mobile applications* the emphasis is on the reduced height, size and the ruggedness of the antenna, for manpack applications it is only important to have a rugged and small size collapsed antenna.

25X1

5 CONCLUSIONS

In a given point-to-point link, the success of meteor scatter communication is largely dependent on the antenna system. Thus, base station as well as out-station antennas need to be considered in this respect. The work presented in this dissertation, however, is concerned only with the investigation of simple out-station antennas which are suitable for mobile and manpack applications.

5.1 Summary Of Findings And Conclusions

5.1.1 Antennas for MBC

The basic concepts of MBC, introduced in chapter 2, underlines the importance of the role played by the antenna system in the meteor scatter environment. Directional properties are exhibited by the geometry of the link, the reflection mechanisms of meteor scatter propagation; and the dependence of trail detection on the illumination of certain sky regions. These directional properties are directly related to the antenna system employed. Hence, the antenna's polarization, radiation pattern, gain and attitude effects the performance of the MBC link. To maximize throughput, all regions of sky which contribute to MBC should be illuminated with high gain antennas.

5.1.2 Antenna design considerations

A logical extension was therefore to examine the principle factors governing the behaviour of simple antennas and the effect of noise on the system. The requirement of simple antenna systems inevitably results in MBC systems of degraded performance due to their reduced size and complexity. The onus is thus placed on the directional master station to provide adequate illumination of sky regions connecting remote stations. The effect of noise on MBC links is to decrease the number of detectable trails as well as the usable signal duration, since signal duration is determined by the period during which the signal-to-noise ratio is above some predefined limit. Unfortunately, noise cannot be completely eliminated, but its introduction via the antenna's beam can be reduced.

Simple antennas are generally defined in this dissertation as those complying with severe size and complexity limitations. However, a simple antenna suitable for mobile applications differs from that which is suitable for a manpack or any other application.

In chapter 3, the value systems for the remote environments of interest are formulated. The value systems enumerate all that is necessary to ensure best value for money in terms of priority and weighting in the antenna design phase. It furnishes a concise specification of the antenna required for any specific application.

Knowing what sort of antennas are required paves the way for their synthesis, evaluation and the prediction of their effect on MBC link performance. In chapter 3 the computer aided antenna analysis tool, NEC2, which is incorporated within the MBC predictive model code, METEOR, is described. These computer based codes, as well as the value systems derived for manpack and mobile applications, are used as engineering tools in the investigation of simple out-station antennas for MBC (outlined in chapter 4). But before particular designs of antennas were appraised in the meteor scatter environment, it was important to establish the effect of different types of sky illumination schemes on MBC link performance. This information, as generalized as it may be, is vital for the design of any antenna for MBC. Hence, a clear categorisation of the link type is furnished in terms of its illumination capability.

For this investigation of the relationships between antenna beamwidth/gain and orientation to the MBC link performance, idealized radiation patterns were synthesized. These ideal patterns were used in the simulation of different illumination schemes. The results, presented in chapter 3, support what is already deduced from the theory (in chapter 2) with regard to the importance of the master station illumination when simple out-station antennas are used. While simple out-station mobile antennas may be of limited directionality, a directional base station concentrating its radiated power on those regions of sky which contribute most to the duty cycle of an MBC link (the "hot spots") will result in dramatic link improvement. Best connectivity is achieved when both ends of the link direct their beams at the hot spots, but this requires complex antennas at the two ends. For each type of illumination scheme there is a trade-off between beamwidth (which is related to the antenna's gain) and throughput. Reducing the antenna's beamwidth (while increasing its gain) results in the illumination of a reduced volume of sky with increased intensity. Up to a certain beamwidth (which is link dependent) this effect improves the throughput. Beyond that point, further reduction of the beamwidth will degrade the throughput.

The indicated optimum master station antenna illumination is not unrealistic since an array of 8 Yagi-Uda antennas with 5 elements each produces approximately 21dBi gain. For networking applications, though, steerable arrays or other versatile solutions should be sought. However, antenna design for master stations is outside the scope of this work.

5.1.3 Simple antennas in the meteor scatter environment

In chapter 4, the electrical performance of simple antennas was evaluated using the NEC2 code. The resulting radiation patterns of these antennas were used to predict, using the prediction software METEOR, the effect of these simple antennas on MBC link throughput for station separation ranging from 100km to 2000km. Both optimum antenna beaming as well as worst case beaming was used in this evaluation.

The purpose of this investigation was to establish bench-mark performance guide for MBC links using simple out-station antennas with emphasis on mobile and manpack applications. The relative performance of MBC links employing three traditional antennas were evaluated in addition to particular designs for mobile and manpack applications. The traditional antennas chosen were the half-wave dipole, the quarter-wave monopole and a 5 element Yagi-Uda antennas. For mobile and manpack applications, a square loop and a long wire antenna was designed and evaluated respectively.

The quarter-wave monopole and the square loop are practical mobile antennas. Theoretical results indicate that at short ranges (up to about 500km) the square loop antenna will offer improved connectivity. Owing to the inability of the loop antenna to illuminate sufficient useful sky regions at larger station separation, the quarter-wave monopole will enhance communications. Both antennas, however, are modelled on an infinite conducting ground plane. In practice, the ground plane is finite and hence slightly different performance to that indicated is expected. The effect of mounting the square loop above a finite conducting plane (such as the roof of a truck) will be to illuminate a larger volume of sky at the expense of upward gain. This should effectively improve communications as range increases since more sky regions will be illuminated. The effect of a finite conducting plane on the monopole antenna is to reduce its forward gain and thereby degrade the overall performance of the link.

Considerably improved throughput can be achieved with a long wire manpack antenna compare to that which is attainable using the mobile antennas described. This is due to the differences in the requirements indicated in the value systems established for remote mobile and manpack antenna systems. While for mobile applications the emphasis is on the reduced height, size and the ruggedness of the antenna, for manpack use it is only important to have a lightweight, rugged and small size collapsed antenna. In fact, for manpack applications the entire communication set must be lightweight as it has to be carried on one's back. Mobile stations are not constrained by weight and hence their transmit power capability can be increased to enhance throughput. The improved performance of the manpack antenna thus compensates for power restrictions on the manpack out-station.

5.2 Proposal For Further Investigation

The work presented in this dissertation is limited to the theoretical investigation of simple meteor scatter out-station antennas. The theoretical results obtained by performing computer simulations of physical systems are only as reliable as their mathematical approximations, coupled with the constraints imposed by the numerical limitations. It is recommended that the theoretical results obtained be validated by measurements. However, in terms of the statement of the problem set to be examined in this dissertation, the effect of different illumination schemes on MBC link performance is established. Different illumination schemes may be dictated for different links such as mobile-to-mobile, manpack-to-manpack, mobile-to-base station, manpack-to-base station etc. Nevertheless, the relative performance associated with these schemes for MBC are indicated. In addition, designs of simple antennas can be assessed with reference to the bench-mark results presented here.

It is envisaged that subsequent work will concentrate on validation of the theoretical results by measurements of simple antennas and MBC link performance. Due to the importance of the master station discussed previously, further work should be carried out on their design and evaluation. Validation of theoretical results will provide the confidence needed to ensure that these form a solid base for further design.

APPENDIX A - THE PROCEDURE OF VALUE ANALYSIS

The value analysis is performed as shown in figure (A-1):

MOBILE REMOTE STATION										
	FUNCTION	COMPARISON							TOTAL
A	Small size of set	A	B_3	C_2	D_3	E_1	F_1	G_1	0
B	Ruggedness of antenna		B	B_1	D_1	B_2	B_2	B_1	9
C	Reduced size of antenna			C	D_2	C_2	F_1	G_1	4
D	Reduction in height of antenna				D	D_3	D_1	D_1	11
E	Limit No of antennas to one only					E	F_2	G_3	1
F	Large messages						F	G_2	4
G	Short waiting time between messages							G	7

FIGURE A-1: Relative importance decision making table.

Importance index:

3 - Much more important

2 - More important

1 - Not much more important

The first entry "B_3" indicate that the ruggedness of the antenna is much more important than having a set of reduced size. In a similar fashion the rest of the table is completed. The numbers associated with each letter are then summed across the matrix and entered in the "TOTAL" column on the right. These could then be normalized with respect to the highest score, multiplied by a factor of 10 or 100 for convenience, and plotted as shown in figure (A-2)

It can be seen from the plot in figure (A-2) that the reduced height of the antenna, which is the most important aspect, can be fulfilled by designing a high power system, thereby increasing the total value of the system. This, of course, would result in a large set. But as indicated, the size of the mobile remote station set is of least importance.

Generally, the designer may use this graph to group the individual aspects into higher order units. Ordinarily, the resulting unit of lower weighting is that which degrades the worth of the system. The elimination of aspects within that unit is often possible by implementing functions within a higher weighting unit differently. This iterative process is carried out to enhance the system's worth.

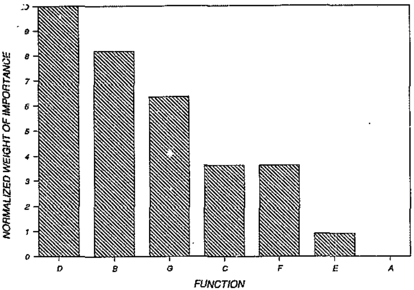

FIGURE A-2: A graphical view of the relative importance for a mobile remote out-station antenna system.

Finally, any design of a system can be evaluated on the basis of how well the requirements, laid down by the value system, are fulfilled using a rating system as shown in figure (A-3)

FUNCTION	B	C	D	E	F	G	TOTAL
NORMALIZED WEIGHT OF IMPORTANCE	8.2	3.6	10.0	0.9	3.6	6.4	-
RATING	3	4	2	4	3	3	-
COMPOUND RATING	24.6	14.4	20.0	3.6	10.8	19.2	92.6

5 - EXCELLENT
4 - VERY GOOD
3 - GOOD
2 - FAIR
1 - POOR

FIGURE A-3: A rating system for any specific design.

The normalized weight of importance values corresponds to those presented in figure (A-2). Any *designed system can then be rated on the basis* of the individual aspects. The compound rating of each functional aspect is the multiplication of the normalized weight of importance of each aspect by the rating of the implementation of that functional aspect. Clearly, the higher total score of the compound rating indicates a better design.

APPENDIX B - THEORY AND IMPLEMENTATIONS OF THE METHOD OF MOMENTS

The Method of Moments is a technique used for the simulation of antennas. This technique, which solves Maxwell's equations numerically for cylindrical wire structures and surfaces, is reviewed in [12]. This technique is in general applicable to conducting bodies with current distribution, J, as shown in figure (B-1). Of particular interest is the current distribution along a thin wire as shown in figure (B-2).

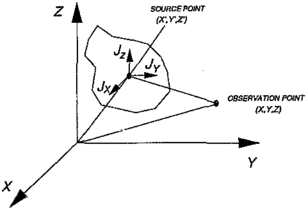

FIGURE B-1: General radiating body.

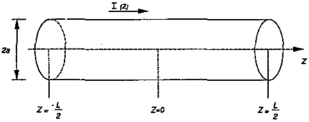

FIGURE B-2: A thin cylindrical wire.

Assuming the wire radius to be much smaller than the wavelength implies that current flows axially only. At the surface of the conducting wire, the electric field boundary condition states that the tangential field component is zero. That is:

$$E_Z^i + E_Z^s = 0 \qquad \text{(B-1)}$$

where E_Z^s is the tangential component of the scattered electric field radiated by J, and E_Z^i is the tangential incident (or impressed) component of the electric field due to some source of excitation. It can be shown [56] that Pocklington equation may be written as:

$$-E_Z^i = \frac{1}{j\omega\varepsilon_0}\int_{-L/2}^{L/2} I(Z')\left(\frac{\partial^2\Phi(Z,Z')}{\partial Z^2} + \beta^2\Phi(Z,Z')\right)dZ' \qquad \text{(B-2)}$$

Where:

$I(Z')$ denotes the current.

$\beta = \omega\sqrt{\mu\varepsilon}$ is the phase constant.

$\Phi(Z,Z')$ is the free space Green's function given by:

$$\Phi(Z,Z') = \frac{1}{4\pi R}e^{-j\beta R} \qquad \text{(B-3)}$$

where R is the distance between the two points (X, Y, Z) and (X', Y', Z') given by :

$$R = \sqrt{(X-X')^2 + (Y-Y')^2 + (Z-Z')^2} \qquad \text{(B-4)}$$

For simplicity, equation (B-2) may be written as:

$$-E_Z^i = \int_{-L/2}^{L/2} I(Z')K(Z,Z')dZ' \qquad \text{(B-5)}$$

The solution obtained for $I(Z')$ is obtained by using the Method of Moments as follows:

Consider the approximation of the current by a series of expansion functions, F_n, such that:

$$I(Z') = \sum_{n=1}^{N} I_n F_n(Z') \qquad \text{(B-6)}$$

where I_n's are complex expansion coefficients.

For simplicity, consider a set of pulse functions:

$$F_n = 1 \quad \text{for } Z' \in \Delta Z'_n \qquad \text{(B-7)}$$

$$= 0 \quad \text{elsewhere}$$

where the wire is divided into N segments of length ΔZ_n. Thus on substitution into equation (B-5):

$$-E^i_Z \cong \int_{-L/2}^{L/2} \sum_{n=1}^{N} I_n F_n(Z') K(Z_m, Z') d Z' \qquad \text{(B-8)}$$

where m indicates that the integral equation is being enforced at m. Thus:

$$-E^i_Z(Z_m) \cong \sum_{n=1}^{N} I_n \int_{\Delta Z'_n} K(Z_m, Z') d Z' \qquad \text{(B-9)}$$

Defining:

$$f(Z_m, Z'_n) = \int_{\Delta Z'_n} K(Z_m, Z') d Z' \qquad \text{(B-10)}$$

Thus:

$$-E^i_Z(Z_m) \cong \sum_{n=1}^{N} I_n f(Z_m, Z'_n) \qquad \text{(B-11)}$$

$$\cong I_1 f(Z_m, Z'_1) + I_2 f(Z_m, Z'_2) + \ldots + I_N f(Z_m, Z'_N)$$

Which in general can be written as:

$$\sum_{n=1}^{N} Z_{m,n} I_n = V_m \qquad \text{(B-12)}$$

where:

$$Z_{m,n} = f(Z_m, Z_n')$$

and

$$V_m = -E_Z^i(Z_m)$$

Equation (B-12) has N unknowns. We therefore require N such equations for a solution to be acquired. This can be achieved by enforcing the integral equation at N points on the wire. This process is called "Point Matching" which is a special case of the Method of Moments.
Hence :

$$[Z_{m,n}]\,[I_N] = [V_m] \qquad \text{(B-13)}$$

Where:

$$[Z_{m,n}]\,[I_N] = \begin{pmatrix} I_1 f(Z_1, Z_1') & I_2 f(Z_1, Z_2') & \dots & I_N f(Z_1, Z_N') \\ I_1 f(Z_2, Z_1') & I_2 f(Z_2, Z_2') & \dots & I_N f(Z_2, Z_N') \\ \vdots & \vdots & & \vdots \\ I_1 f(Z_N, Z_1') & I_2 f(Z_N, Z_2') & \dots & I_N f(Z_N, Z_N') \end{pmatrix}$$

and

$$[V_m] = \begin{pmatrix} -E_Z^i(Z_1) \\ -E_Z^i(Z_2) \\ \vdots \\ -E_Z^i(Z_N) \end{pmatrix}$$

Therefore:

$$[I_N] = [Z_{m,n}]^{-1}\,[V_m] \qquad \text{(B-14)}$$

where:

$[I_N]$ is a column vector of generalized currents.

$[Z_{m,n}]$ is a matrix of generalized impedances.

$[V_m]$ is a column vector of generalized voltages.

Clearly, this derivation assumes only a single wire on the Z-axis, but could be extended to arbitrarily orientated wires interacting with each other. The special case of Point Matching can be viewed as a relaxation of the boundary conditions such that it is only satisfied at a specific point. In between these points we can only hope that the boundary conditions are not so badly violated that the solution *is not useful.*

The more general method is derived by considering the so called "Residual", R(Z), as:

$$R(Z) = E_Z^s + E_Z^i \qquad \text{(B-15)}$$

Clearly, we wish R(Z) to be zero in order to satisfy boundary conditions. Hence:

$$R(Z) = \sum_{n=1}^{N} I_n f(Z, Z_n') + E_Z^i(Z) \qquad \text{(B-16)}$$

This equation evaluated at $Z = Z_n$ gives the residual $R(Z_n)$ at the n^{th} point where it must clearly be zero. However, at other points the residual electric field may not be zero. In the method of weighted residuals, the current are found such that *R(Z) is forced to be zero in the average sense*, by means of weighted functions $W_m(Z)$. i.e.:

$$\int W_m(Z) R(Z) d\,Z = 0 \qquad \text{(B-17)}$$

$$m = 1 \ldots N$$

Hence, substituting for R(Z), we can write the integral equation as:

$$\int_{-L/2}^{L/2} W_m(Z) \sum_{n=1}^{N} I_n f(Z, Z_n') d\,Z + \int_{-L/2}^{L/2} W_m(Z) E_Z^i(Z) d\,Z = 0 \qquad \text{(B-18)}$$

If we use impulse weighting functions:

$$W_m(Z) = \delta(Z - Z_m) \qquad \text{(B-19)}$$

with pulse testing functions where $\delta(Z-Z_m)$ are the Dirac-delta functions, then substitution into equation (B-18) yields:

$$\sum_{n=1}^{N} I_n f(Z_m, Z_n') = -E_Z^i(Z_m) \qquad \text{(B-20)}$$

which is the special case of Point Matching as shown above. However, if alternatively we define W_m to be pulse functions:

$$W_m = 1 \quad \text{for } Z \in \Delta Z_m \qquad \text{(B-21)}$$

$$= 0 \quad \text{elsewhere}$$

with pulse testing functions, then we obtain what is known as a "Galerkin Method", i.e.:

$$\sum_{n=1}^{N} I_n \int_{\Delta Z_n} f(Z, Z_n') dZ + \int_{\Delta Z_m} E_Z^i(Z) dZ = 0 \qquad \text{(B-22)}$$

$$m = 1 \ldots N$$

The Method of Moments is therefore equivalent to the method of weighted residuals and the choice of expansion and weighting functions ultimately determines the value of the specific method.

NEC2 utilizes the Pocklington integral equation for currents on thin wires. NEC2 analysis is carried out using the "point matching" Method of Moments technique which uses the Dirac delta functions as weighting functions and a three term function for test functions. These three terms consist of the sum of a Sine, Cosine and a constant term. In the Method of Moments computer time is proportional to the third power of the number of segments thereby limiting the possible size of structures that may be analysed.

APPENDIX C - NUMERICAL MODELLING CONSTRAINTS AND LIMITATIONS

The mathematical modelling of the antenna and its environment is the most important aspect of simulation where accurate results of performance are desired. This together with the constraints and limitations of the particular method of analysis used, coupled with the computer capabilities determines the accuracy of the evaluation.

The Method of Moments, presented in Appendix B, assumes all wires to have a radius which is much smaller than the wavelength. This implies that current flows in the axial direction only since the Method of Moments does not account for circulating currents. As a result of this the ratio of wire radius to wavelength, the ratio of segments length to radius and the number of segments per wavelength are parameters on which some limit is imposed [12].

The effect of mutual interaction between the antenna and its environment must not be overlooked. A common environmental effect on antennas, especially at lower frequencies, is the earth above which the structure is erected. Hansen [57] demonstrated the following effect of different ground planes on the antennas performance : The effect of power lost into an imperfect earth becomes independent of the height once the antenna is higher than about 0.2 wavelengths above ground level. This finding implies that antennas can be compared in terms of structure efficiency once it is erected higher than 0.2 wavelength above the earth.

Another important aspect in antenna modelling, especially for the purpose of complex structure simplification, is the effect of the wire length. It has been demonstrated by Fourie [55] that the physical length of a wire between discontinuities is retained as long as the angle between sections does not exceed a certain limit. The validation of this finding is illustrated in figure (C-1) [adapted from ref. 58]. Figure (C-1) shows the model on which simulation was performed and the investigation results of the extent to which the wire length, rather than the dimensions measured in a straight line, is the predominant factor in antenna performance.

For evaluation using the NEC2 code, a wire is defined by its radius and the coordinates of its two end points. The wire consists of straight segments following its path in a piece-wise linear fashion. Generally, a segment length should be less than 0.1 of a wavelength and greater than 0.001 of a wavelength at the desired frequency of analysis.

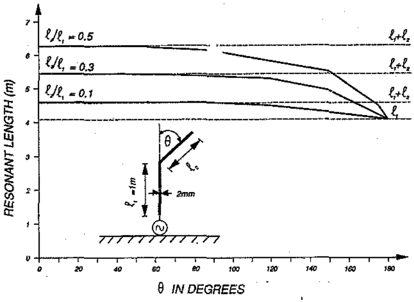

FIGURE C-1: The graph of antenna resonant wavelength versus the angle with the vertical, θ.

The Method of Moments technique used considers only current flow in the axial direction on a segment. The acceptability of these approximations is dependent on the wire radius such that unless the ratio of wire radius to wavelength is much less than $1/(2\pi)$, the validity of these approximations is not necessarily accurate.

The accuracy of the numerical solution for axial currents is also dependent on the ratio of segment length to wire radius. This ratio must be greater than 8 in order to achieve errors of less than 1 percent, using the standard thin wire kernel, and may be as small as 2, if the extended thin wire kernel is used.

Segments are treated as connected when the separation of their ends is less than 0.001 times the length of the shortest segment.

Maintenance of current continuity across wire junction presents another limitation since antennas with short sections of wire coupled to long ones require exceedingly large number of segments to be analysed [58]. Kubina's rule of thumb states that "The restriction on the relative length of segments that form a junction, require that these lengths be comparable within a factor of five" [59]. Further more, the number of wires joined at a single junction cannot exceed 30 due to a dimension limitation in the NEC2 code.

Kubina's rule of thumb, which can be viewed in conjunction with figure (C-2), states that the restriction on the relative length of segments that form a junction is given by:

$$5 > \left(\frac{\Delta_1}{\Delta_2}\right) > \frac{1}{5} \qquad \text{(C-1)}$$

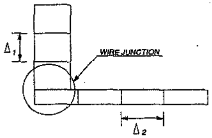

FIGURE C-2: Two wire junction.

A conducting surface is modelled by means of multiple, small flat surface patches corresponding to segments used to model wires. The patches are specified such that they cover the entire surface to be modelled. The parameters defining a surface patch are the cartesian coordinates of the patch centre, the component of the outward directed unit normal vector and the patch area.

For accuracy of results, a minimum of 25 patches per square wavelength of surface area should be used and the maximum size of an individual patch should not exceed 0.04 square wavelengths.

Since the division of current between two overlapping segments or patches is indeterminate, segments or patches may not overlap.

The radius of tapered wires may not change drastically since a large radius change between connected segments may decrease accuracy. This rule particularly applies where the ratio of segment length to radius is small.

A segment must exist at each point where a network connection or voltage source will be positioned. This constraint is imposed so that voltage drop can be specified as a boundary condition.

Finally, the order in which the various cards are specified must obey some rules which are imperative for a successful run of the NEC2 code. Generally, the card deck begins with cards containing comments made by the user. These are followed by geometry data cards specifying the geometry of the antenna and thereafter the program control cards, specifying electrical parameters and requests for the computation of antenna characteristics.

The above does not attempt to cover all the modelling constraints which are imposed by the NEC2 code but only to highlight a cross section of them. This is carried out in the hope of conveying the complexity which is involved with structure modelling, such that meaningful evaluation results may be obtained. Furthermore, numerical evaluation of the performance of antennas, using the Method of Moments would be more erroneous when computing parameters such as input impedance rather than integrated quantities such as efficiency, radiation pattern or gain [59]. This is due to the fact that the input impedance calculation is based on the absolute value of current at the feed point. Subsequent integration has a smoothing effect thus reducing the error. Hence, measured results which compare well with the computed input impedance may serve as a good indication as to the validity of the numerical model employed.

APPENDIX D - PREDICTION MODEL SETTINGS FOR MBC LINK SIMULATION

The detailed description of the MBC link and the various parametric settings of the prediction model, METEOR [13], used for the investigation discarded in section 3.3 is as follows:

```
Meteor Scatter Prediction System    Ver 1.10  P.J.Rodman/J.D.Larsen  1987/8

              System:TEST,Rx:R1,Tx:T4,Earth:TEST,Protocol:TEST
                    Distn:TEST,Noise:TEST,Var: nD (qmus)

                            Earth Environment

A: Path Length:                                   533.4 km
B: Local Time:                                  6:00:00
C: Date:                                       13/12/87    (Day: 307)
D: X From:                                       -300.0 km
E: X To:                                          300.0 km
F: Y From:                                       -300.0 km
G: Y To:                                          300.0 km
H: Grid Cell Size:                                 10.0 km
I: Receiver Latitude:                         -30:00:00 ( )
J: Receiver Longitude:                         31:00:00 (LST: 11:25:14)
K: Receiver Direction from North:                 -34.2 deg
L: Transmitter Latitude:                      -26:00:00 ( )
M: Transmitter Longitude:                      28:00:00 (LST: 11:13:14)
N: Transmitter Direction from North:              147.2 deg
O: Offset of Local Time from GMT:                   2.0 hours
No. of Rx Obstacles: 0      No. of Tx Obstacles: 0
```

Meteor Scatter Prediction System   Ver 1.10 P.J.Rodman/J.D.Larsen 1987/8

System:TEST,Rx:R1,Tx:T4,Earth:TEST,Protocol:TEST
Distn:TEST,Noise:TEST,Var: nD (qmus)

System Environment

A: Transmit Power:	400.0 W
B: Wavelength (Frequency):	6.000 m (50.000 MHz)
C: Polarisation:	Horizontal
D: No. of Integration Intervals:	20
E: Earth Shape:	Round
F: Theory:	Meeks and James
G: Illumination used:	Yes
H: Maximum/Minimum/Sum/Average:	Maximum
I: Polarisation used:	Yes
J: Hmi setting:	0.0 km
K: Height - Lower Limit:	98.0 km
L: Height - Upper Limit:	102.0 km
M: Calculation Gain Boundary:	20.0 dB
N: Calculate Pm using Bit Error Rate:	No
O: Use Orbital/Radiant Distn.:	No
P: No. of Height Intervals (Larsen):	0

Meteor Scatter Prediction System   Ver 1.10 P.J.Rodman/J.D.Larsen 1987/8

System:TEST,Rx:R1,Tx:T4,Earth:TEST,Protocol:TEST
Distn:TEST,Noise:TEST,Var: nD (qmus)

Distribution Environment

A: Tmin:	60.00 msec
B: Time Constant Type:	Time Constant Slope
C: Time Constant Distn. Measured Data File:	<Unknown>
D: Time Constant Distribution - From:	0.010
E: Time Constant Distribution - To:	0.300
F: Time Constant Distribution - Increment:	0.010
G: Velocity Distn. Measured Data File:	<Unknown>
H: Velocity Distribution - From:	10.000 km/s
I: Velocity Distribution - To:	70.000 km/s
J: Velocity Distribution - Increment:	2.000 km/s
K: Height Distn. Measured Data File:	<Unknown>
L: Height Distribution - From:	80.000 km
M: Height Distribution - To:	110.000 km
N: Height Distribution - Increment:	1.000 km

```
Meteor Scatter Prediction System    Ver 1.10  P.J.Rodman/J.D.Larsen  1987/8

              System:TEST,Rx:R1,Tx:T4,Earth:TEST,Protocol:TEST
                   Distn:TEST,Noise:TEST,Var: nD (qmus)

                            Noise Environment

A: System Bandwidth:                          8000.0 Hz
B: Noise Floor:                             (Predicted) dBm
C: Minimum Detectable Signal/Noise:             10.0 dB (above noise)
D: Ambient Temperature (K):                    300.0 K
E: Ambient Temperature (C):                     27.0 C
F: System Feeder Loss:                           1.0
G: System Feeder Loss (dB):                      0.0 dB
H: Receiver Noise Figure:                        1.9
I: Receiver Noise Temperature:                 270.0 K
J: Environmental Noise Temperature:              0.0 K
K: Environmental Noise Power:                 -330.0 dBm
No. of Rx Noise Sources:        0     No. of Tx Noise Sources:        0
Total Rx Computed Power:      N/A     To[illegible] Tx Computed Power:      N/A
```

```
Meteor Scatter Prediction System    Ver 1.10  P.J.Rodman/J.D.Larsen  1987/8

              System:TEST,Rx:R1,Tx:T4,Earth:TEST,Protocol:TEST
                   Distn:TEST,Noise:TEST,Var: nD (qmus)

                              Constants A

A: k:                                            1.40
B: Length of Tr[illegible] Zenith (Ltz):             15.00 km
C: K (06h00):                                4.3E-0001
D: K (18h00):                                5.0E+0002
E: k2:                                       5.0E-0023
F: Height:                                      97.0 km
G: Velocity/Height Slope:                     0.3300
H: Velocity/Height Intercept:                  80.00 km
I: Transition Line Density (qT):             2.0E+0024 e/m
J: Multiplier:                               9.3E+0008
K: k3:                                           5.0
L: Heliocentric Velocity (Vh):                  40.0 km/s
M: k4:                                           0.0
N: Velocity Calculation:                       Vh/Ve
O: Velocity/Height Relationship:              Linear
P: Temperature Conversion factor:               2.40
Q: Use Annual Cycle Info:                         No
```

```
Meteor Scatter Prediction System    Ver 1.10  P.J.Rodman/J.D.Larsen  1987/8

              System:TEST,Rx:R1,Tx:T4,Earth:TEST,Protocol:TEST
                    Distn:TEST,Noise:TEST,Var: nD (qmus)

                              Constants B

A: Davies' Radiant Distn. Big K Multiplier:          0.0
B: Rudie's Orbital Distn. Big K Multiplier:          0.0
C: Diff.Coeff. A:        6.70  D: Diff.Coeff. B:     5.60
E: r0.Coeff. A:          7.50  F: r0.Coeff. B:       7.20
G: Rudie's Xi:                                       0.0 deg
H: Rudie's Delta S:                                  0.0 deg
I: Rudie's Tilt (d):                                 0.0 deg
J: Rudie's Orbital Distn. Count Multiplier:          0.0
K: Rudie's Pole Angle:                               0.0 deg
L: Rudie's xtl Case:                               -ve Case
M: Rudie's xtl Negation:                           No Change
N: Rudie's +ve Case From:                            0.00*pi
O: Rudie's +ve Case To:                              0.00*pi
P: Use Rudie's...:                                   None
Q: Rudie's Criterion Bound:                         0.0E+0000
R: Rudie's Orbit Selection:                         00000000
S: Type of Orbit/Radiant Computation:              Rudie's Orbit
```

```
Meteor Scatter Predictio   tem    Ver 1.10  P.J.Rodman/J.D.Larsen  1987/8

              System:TEST,Rx:R1,Tx:T4,Earth:TEST,Protocol:TEST
                    Distn:TEST,Noise:TEST,Var: nD (qmus)

                              Constants C

A: Radiant Distribution Multipliers:
B: Hawkins' Radiant Distn. Big K Multiplier:         0.0
C: Initial Radius Effect:                          Enabled
D: Trail Formation Effect:                         Enabled
E: Diffusion Effect:                               Enabled
F: Psi m Effect:                                   Disabled
G: Zenith Attraction Cutoff Angle:                  10.0 deg
H: Shower Computation:                             Disabled
I: Shower Big K Multiplier:                          0.0
J: Shower Velocity Multiplier:                       0.0
K: Initial Radius Effect (Showers):                Disabled
L: Trail Formation Effect (Showers):               Disabled
M: Diffusion Effect (Showers):                     Disabled
N: Psi m Effect (Showers):                         Disabled
O: Use Zeta or Z0:                                   Z0
```

Apart for the geographical location of the stations, the same settings were used for the simulations outlined in chapter 4.

APPENDIX E - TABULATED RESULTS

Tabulated results for the investigation of the ***effect of antenna beamwidth/directivity and orientation on MBC*** presented in section 3.3.3:

Type 1 illumination			Type 2 illumination			Type 3 illumination		
D	M/h	DU	D	M/h	DU	D	M/h	DU
9.0	83.8	34.0	16.6	141.0	52.1	16.6	583.3	203.7
9.5	89.8	36.6	17.2	148.8	54.2	17.2	657.3	226.2
10.0	95.8	39.4	17.9	159.4	57.5	17.9	754.2	258.0
10.6	101.1	42.0	18.6	168.3	59.7	18.6	861.0	289.5
11.2	105.5	44.5	19.3	180.8	63.3	19.3	997.5	331.5
11.8	109.8	47.1	20.1	189.3	64.9	20.1	1143.2	373.5
12.5	111.3	48.8	21.0	202.9	68.7	21.0	1286.9	414.0
13.3	111.5	50.2	22.1	207.6	69.1	22.1	1494.5	474.9
14.1	108.3	50.2	23.2	200.7	66.0	23.2	1634.2	511.9
15.0	103.0	49.5	24.6	195.6	63.5	24.6	1858.3	573.9
16.1	95.3	47.4	26.2	180.5	59.8	26.2	1798.0	542.7
17.2	84.7	43.9	28.1	161.9	53.6	28.1	1953.2	608.4
18.6	72.6	39.1	30.6	114.5	39.2	30.6	634.2	190.2
20.1	49.3	29.7	34.1	89.0	30.4			
22.0	15.3	13.9						
24.6	4.1	5.0						
28.1	1.0	1.5						

Index:

D = Directivity (dBi).

M/h = Meteors per hour.

DU = Channel duration (Sec/hr).

Type 1, 2 and 3 illuminations are as described in section 3.3.2.

Tabulated results for ***MBC link performance using simple antennas*** presented in chapter 4:

Results for half-wave dipole, *vertical* quarter-wave monopole and 45° skew quarter-wvae monopole (section 4.2.2)

	HWD				QWM		SWQM			
	Best		Worst		Best		Best		Worst	
D	M/h	DU	M/h	DU	M/h	DU	M/h	DU	M/h	DU
100	0.7	0.1	0.2	0.1	0.1	0.1	0.2	0.1	0.2	0.1
200	2.3	0.5	0.5	0.1	1.4	0.3	1.5	0.3	1.4	0.3
300	5.3	1.5	0.6	0.2	3.4	0.9	3.4	0.9	3.0	0.8
400	7.9	3.0	0.4	0.1	3.8	1.3	3.7	1.3	3.1	1.1
500	12.0	5.6	0.3	0.1	4.4	1.8	4.0	1.7	3.4	1.4
600	14.6	8.2	0.3	0.1	3.8	1.9	3.4	1.7	2.8	1.4
700	15.9	10.7	0.2	0.1	3.0	1.7	2.6	1.5	2.2	1.3
800	16.1	12.6	0.1	0.1	2.3	1.5	2.0	1.3	1.7	1.1
900	15.2	13.7			1.8	1.3	1.8	1.3	1.3	1.1
1000	13.5	13.9			1.3	1.1	1.4	1.1	0.9	0.7
1100	12.1	14.0			1.2	1.0	1.1	0.9	0.9	0.6
1200	8.8	11.7			0.7	0.7	0.7	0.6	0.6	0.5
1300	6.6	9.9			0.5	0.6	0.4	0.5	0.3	0.4
1400	4.5	7.5			0.3	0.4	0.2	0.3	0.2	0.3

remainder of table on next page...

	HWD				QWM		SWQM			
	Best		Worst		Best		Best		Worst	
D	M/h	DU	M/h	DU	M/h	DU	M/h	DU	M/h	DU
1500	3.0	5.5			0.2	0.3	0.1	0.2	0.1	0.2
1600	1.9	3.9			0.1	0.2	0.1	0.1	0.1	0.1
1700	1.4	3.0			0.1	0.1				
1800	0.7	1.7								
1900	0.4	1.1								
2000	0.2	0.5								

<u>Index:</u>

HWD = Half-wave dipole.

QWM = Quarter-wave monopole.

SQWM = 45° skew quarter-wave monopole.

Best = *Best orientation* of antenna.

Worst = Worst orientation of antenna.

D = Stations separation (km).

M/h = Meteors per hour.

DU = Channel duration (sec/hr).

Tabulated results for the square loop antenna presented in section 4.3:

	SLOOP (MID-PATH)				SLOOP (END-PATH)			
	Best		Worst		Best		Worst	
D	M/h	DU	M/h	DU	M/h	DU	M/h	DU
100	2.7	0.4	1.5	0.2	2.6	0.4	1.5	0.2
200	4.8	0.9	2.4	0.4	4.8	0.9	2.5	0.5
300	6.3	1.6	2.9	0.7	6.2	1.5	3.1	0.7
400	5.3	1.7	2.0	0.5	5.3	1.6	2.1	0.5
500	4.8	1.9	1.4	0.4	4.8	1.8	1.4	0.4
600	3.6	1.6	0.9	0.3	3.7	1.6	0.9	0.3
700	2.6	1.2	0.5	0.2	2.6	1.2	0.6	0.2
800	1.8	0.9	0.3	0.1	1.8	0.9	0.4	0.1
900	1.2	0.6	0.2	0.1	1.2	0.6	0.2	0.1
1000	0.8	0.4			0.8	0.4		
1100	0.5	0.3			0.5	0.3		
1200	0.1	0.1			0.1	0.1		

Index:

SLOOP = Square loop antenna.

MID-PATH = Mid-path illumination by the Yagi-Uda antenna at the other end of the link.

END-PATH = End-path illumination by the Yagi-Uda antenna at the other end of the link.

Best = Best orientation of squar loop antenna.

Worst = Worst orientation of square loop antenna.

D = Stations separation (km).

M/h = Meteors per hour.

DU = Channel duration (Sec/hr).

Tabulated results for the Yagi-Uda and *long wire* (*terminated*) antennas presented in section 4.4:

	LONG-WIRE		YAGI-UDA	
D	M/h	DU	M/h	DU
100	1.7	0.3	4.7	0.7
200	4.7	0.9	11.0	2.2
300	13.2	3.5	24.7	6.7
400	28.0	9.6	44.0	15.1
500	44.1	17.1	68.3	28.5
600	64.2	29.6	91.2	44.7
700	77.0	41.3	111.8	62.7
800	79.8	46.1	128.4	81.1
900	85.6	61.5	139.9	98.3
1000	88.9	70.3	147.1	113.5
1100	80.0	62.6	149.7	125.8
1200	71.6	60.7	145.5	133.0
1300	61.5	56.4	134.0	133.9
1400	49.3	49.0	116.8	127.4
1500	34.9	37.6	89.8	104.8

remainder of table *on next page*...

	LONG-WIRE		YAGI-UDA	
D	M/h	DU	M/h	DU
1600	18.4	22.0	66.6	86.9
1700	9.3	12.0	48.9	68.9
1800	5.5	7.5	32.0	48.9
1900	2.2	3.2	19.5	32.2
2000	0.3	0.6	10.5	18.8

<u>Index:</u>

LONG-WIRE = Long wire (terminated) antenna.

YAGI-UDA = Yagi- Uda antenna.

D = Stations separation (km).

M/h = Meteors per hour.

DU = Channel duration (Sec/hr).

Zenith-plane radiation pattern of the 5-elements Yagi-Uda antenna.

ANGLES		DIRECTIVE GAINS		
Theta	Phi	Vertical	Horizontal	Total
Degrees	Degrees	dB	dB	dB
0	90	-99.31	-1.46	-1.46
4	90	-99.33	-2.31	-2.31
8	90	-99.39	-3.69	-3.69
12	90	-99.49	-5.9	-5.9
16	90	-99.64	-9.52	-9.52
20	90	-99.83	-15.34	-15.34
24	90	-100.06	-13.11	-13.11
28	90	-100.35	-6.92	-6.92
32	90	-100.69	-2.89	-2.89
36	90	-101.1	-0.04	-0.04
40	90	-101.56	2.11	2.11
44	90	-102.1	3.8	3.8
48	90	-102.72	5.16	5.16
52	90	-103.44	6.26	6.26
56	90	-104.27	7.16	7.16
60	90	-105.24	7.9	7.9
64	90	-106.38	8.5	8.5
68	90	-107.75	8.99	8.99
72	90	-109.42	9.37	9.37

76	90	-111.54	9.66	9.66
80	90	-114.42	9.87	9.87
84	90	-118.83	10.01	10.01
88	90	-128.36	10.08	10.08
92	90	-128.36	10.08	10.08
96	90	-118.83	10.01	10.01
100	90	-114.42	9.87	9.87
104	90	-111.54	9.66	9.66
108	90	-109.42	9.37	9.37
112	90	-107.75	8.99	8.99
116	90	-106.38	8.5	8.5
120	90	-105.24	7.9	7.9
124	90	-104.27	7.16	7.16
128	90	-103.44	6.26	6.26
132	90	-102.72	5.16	5.16
136	90	-102.1	3.8	3.8
140	90	-101.56	2.11	2.11
144	90	-101.09	-0.04	-0.04
148	90	-100.69	-2.89	-2.89
152	90	-100.35	-6.92	-6.92
156	90	-100.06	-13.11	-13.11
160	90	-99.83	-15.34	-15.34
164	90	-99.64	-9.52	-9.52

168	90	-99.49	-5.9	-5.9
172	90	-99.39	-3.69	-3.69
176	90	-99.33	-2.31	-2.31
180	90	-99.31	-1.46	-1.46
184	90	-99.32	-1.02	-1.02
188	90	-99.39	-0.88	-0.88
192	90	-99.49	-1	-1
196	90	-99.64	-1.32	-1.32
200	90	-99.83	-1.81	-1.81
204	90	-100.07	-2.44	-2.44
208	90	-100.36	-3.16	-3.16
212	90	-100.71	-3.96	-3.96
216	90	-101.12	-4.81	-4.81
220	90	-101.59	-5.68	-5.68
224	90	-102.13	-6.58	-6.58
228	90	-10..76	-7.5	-7.5
232	90	-103.49	-8.47	-8.47
236	90	-104.32	-9.48	-9.48
240	90	-105.3	-10.56	-10.56
244	90	-106.44	-11.69	-11.69
248	90	-107.81	-12.88	-12.88
252	90	-109.48	-14.08	-14.08
256	90	-111.61	-15.23	-15.23

260	90	-114.49	-16.24	-16.24
264	90	-118.9	-16.99	-16.99
268	90	-128.43	-17.4	-17.4
272	90	-128.43	-17.4	-17.4
276	90	-118.9	-16.99	-16.99
280	90	-114.49	-16.24	-16.24
284	90	-111.61	-15.23	-15.23
288	90	-109.48	-14.08	-14.08
292	90	-107.81	-12.88	-12.88
296	90	-106.44	-11.69	-11.69
300	90	-105.3	-10.56	-10.56
304	90	-104.32	-9.48	-9.48
308	90	-103.49	-8.47	-8.47
312	90	-102.76	-7.5	-7.5
316	90	-102.13	-6.58	-6.58
320	90	-101.59	-5.68	-5.68
324	90	-101.12	-4.81	-4.81
328	90	-100.71	-3.96	-3.96
332	90	-100.36	-3.16	-3.16
336	90	-100.07	-2.44	-2.44
340	90	-99.83	-1.81	-1.81
344	90	-99.64	-1.32	-1.32
348	90	-99.49	-1	-1

352	90	-99.39	-0.88	-0.88
356	90	-99.32	-1.02	-1.02
360	90	-99.31	-1.46	-1.46

Zenith-plane radiation pattern of the 5-elements Yagi-Uda antenna.

ANGLES		DIRECTIVE GAINS		
Theta	Phi	Vertical	Horizontal	Total
Degrees	Degrees	dB	dB	dB
0	90	-99.31	-1.46	-1.46
4	90	-99.33	-2.31	-2.31
8	90	-99.39	-3.69	-3.69
12	90	-99.49	-5.9	-5.9
16	90	-99.64	-9.52	-9.52
20	90	-99.83	-15.34	-15.34
24	90	-100.06	-13.11	-13.11
28	90	-100.35	-6.92	-6.92
32	90	-100.69	-2.89	-2.89
36	90	-101.1	-0.04	-0.04
40	90	-101.56	2.11	2.11
44	90	-102.1	3.8	3.8
48	90	-102.72	5.16	5.16
52	90	-103.44	6.26	6.26
56	90	-104.27	7.16	7.16
60	90	-105.24	7.9	7.9
64	90	-106.38	8.5	8.5
68	90	-107.75	8.99	8.99
72	90	-109.42	9.37	9.37

76	90	-111.54	9.66	9.66
80	90	-114.42	9.87	9.87
84	90	-118.83	10.01	10.01
88	90	-128.36	10.08	10.08
92	90	-128.36	10.08	10.08
96	90	-118.83	10.01	10.01
100	90	-114.42	9.87	9.87
104	90	-111.54	9.66	9.66
108	90	-109.42	9.37	9.37
112	90	-107.75	8.99	8.99
116	90	-106.38	8.5	8.5
120	90	-105.24	7.9	7.9
124	90	-104.27	7.16	7.16
128	90	-103.44	6.26	6.26
132	90	-102.72	5.16	5.16
136	90	-102.1	3.8	3.8
140	90	-101.56	2.11	2.11
144	90	-101.09	-0.04	-0.04
148	90	-100.69	-2.89	-2.89
152	90	-100.35	-6.92	-6.92
156	90	-100.06	-13.11	-13.11
160	90	-99.83	-15.34	-15.34
164	90	-99.64	-9.52	-9.52

168	90	-99.49	-5.9	-5.9
172	90	-99.39	-3.69	-3.69
176	90	-99.33	-2.31	-2.31
180	90	-99.31	-1.46	-1.46
184	90	-99.32	-1.02	-1.02
188	90	-99.39	-0.88	-0.88
192	90	-99.49	-1	-1
196	90	-99.64	-1.32	-1.32
200	90	-99.83	-1.81	-1.81
204	90	-100.07	-2.44	-2.44
208	90	-100.36	-3.16	-3.16
212	90	-100.71	-3.96	-3.96
216	90	-101.12	-4.81	-4.81
220	90	-101.59	-5.68	-5.68
224	90	-102.13	-6.58	-6.58
228	90	-10[illegible]76	-7.5	-7.5
232	90	-103.49	-8.47	-8.47
236	90	-104.32	-9.48	-9.48
240	90	-105.3	-10.56	-10.56
244	90	-106.44	-11.69	-11.69
248	90	-107.81	-12.88	-12.88
252	90	-109.48	-14.08	-14.08
256	90	-111.61	-15.23	-15.23

260	90	-114.49	-16.24	-16.24
264	90	-118.9	-16.99	-16.99
268	90	-128.43	-17.4	-17.4
272	90	-128.43	-17.4	-17.4
276	90	-118.9	-16.99	-16.99
280	90	-114.49	-16.24	-16.24
284	90	-111.61	-15.23	-15.23
288	90	-109.48	-14.08	-14.08
292	90	-107.81	-12.88	-12.88
296	90	-106.44	-11.69	-11.69
300	90	-105.3	-10.56	-10.56
304	90	-104.32	-9.48	-9.48
308	90	-103.49	-8.47	-8.47
312	90	-102.76	-7.5	-7.5
316	90	-102.13	-6.58	-6.58
320	90	-101.59	-5.68	-5.68
324	90	-101.12	-4.81	-4.81
328	90	-100.71	-3.96	-3.96
332	90	-100.36	-3.16	-3.16
336	90	-100.07	-2.44	-2.44
340	90	-99.83	-1.81	-1.81
344	90	-99.64	-1.32	-1.32
348	90	-99.49	-1	-1

352	90	-99.39	-0.88	-0.88
356	90	-99.32	-1.02	-1.02
360	90	-99.31	-1.46	-1.46

Azimuth-plane radiation pattern of the 5-elements Yagi-Uda antenna.

ANGLES		DIRECTIVE GAINS		
Theta	Phi	Vertical	Horizontal	Total
Degrees	Degrees	dB	dB	dB
90	2	-151.07	-33.47	-33.47
90	6	-152.23	-26.05	-26.05
90	10	-154.13	-23.04	-23.04
90	14	-157.22	-23.1	-23.1
90	18	-162.7	-27.45	-27.45
90	22	-166.53	-33.24	-33.24
90	26	-159	-18.82	-18.82
90	30	-154.26	-12.19	-12.19
90	34	-151.23	-7.69	-7.69
90	38	-149.12	-4.26	-4.26
90	42	-147.63	-1.5	-1.5
90	46	-146.59	0.77	0.77
90	50	-145.93	2.66	2.66
90	54	-145.59	4.26	4.26
90	58	-145.56	5.61	5.61
90	62	-145.85	6.74	6.74
90	66	-146.46	7.67	7.67
90	70	-147.45	8.44	8.44
90	74	-148.91	9.04	9.04

90	78	-151.05	9.5	9.5
90	82	-154.32	9.83	9.83
90	86	-160.2	10.02	10.02
90	90	-999.99	10.08	10.08
90	94	-160.2	10.02	10.02
90	98	-154.32	9.83	9.83
90	102	-151.05	9.5	9.5
90	106	-148.91	9.04	9.04
90	110	-147.45	8.44	8.44
90	114	-146.46	7.67	7.67
90	118	-145.85	6.74	6.74
90	122	-145.56	5.61	5.61
90	126	-145.59	4.26	4.26
90	130	-145.93	2.66	2.66
90	134	-146.59	0.77	0.77
90	138	-147.63	-1.5	-1.5
90	142	-149.12	-4.26	-4.26
90	146	-151.23	-7.69	-7.69
90	150	-154.26	-12.19	-12.19
90	154	-159	-18.82	-18.82
90	158	-166.53	-33.24	-33.24
90	162	-162.7	-27.44	-27.44
90	166	-157.22	-23.1	-23.1

90	170	-154.13	-23.03	-23.03
90	174	-152.23	-26.05	-26.05
90	178	-151.07	-33.47	-33.47
90	182	-150.4	-26.78	-26.78
90	186	-150.12	-20.33	-20.33
90	190	-150.16	-16.6	-16.6
90	194	-150.46	-14.18	-14.18
90	198	-150.98	-12.56	-12.56
90	202	-151.7	-11.47	-11.47
90	206	-152.59	-10.77	-10.77
90	210	-153.61	-10.37	-10.37
90	214	-154.74	-10.19	-10.19
90	218	-155.95	-10.18	-10.18
90	222	-157.25	-10.32	-10.32
90	226	-158.63	-10.57	-10.57
90	230	-160.1	-10.93	-10.93
90	234	-161.7	-11.4	-11.4
90	238	-163.44	-11.97	-11.97
90	242	-165.38	-12.66	-12.66
90	246	-167.53	-13.46	-13.46
90	250	-169.95	-14.33	-14.33
90	254	-172.71	-15.23	-15.23
90	258	-175.94	-16.08	-16.08

90	262	-180.04	-16.8	-16.8
90	266	-186.44	-17.28	-17.28
90	270	-999.99	-17.45	-17.45
90	274	-186.43	-17.28	-17.28
90	278	-180.04	-16.8	-16.8
90	282	-175.93	-16.08	-16.08
90	286	-172.7	-15.23	-15.23
90	290	-169.95	-14.33	-14.33
90	294	-167.53	-13.46	-13.46
90	298	-165.38	-12.66	-12.66
90	302	-163.44	-11.97	-11.97
90	306	-161.7	-11.4	-11.4
90	310	-160.1	-10.93	-10.93
90	314	-158.63	-10.57	-10.57
90	318	-157.25	-10.32	-10.32
90	322	-155.95	-10.18	-10.18
90	326	-154.74	-10.19	-10.19
90	330	-153.61	-10.37	-10.37
90	334	-152.59	-10.77	-10.77
90	338	-151.7	-11.47	-11.47
90	342	-150.98	-12.56	-12.56
90	346	-150.46	-14.18	-14.18
90	350	-150.16	-16.6	-16.6

90	354	-150.12	-20.33	-20.33
90	358	-150.4	-26.78	-26.78
90	362	-151.07	-33.47	-33.47

Azimuth-plane radiation pattern of the half-wave dipole antenna in free space.

ANGLES		DIRECTIVE GAINS		
Theta	Phi	Vertical	Horizontal	Total
Degrees	Degrees	dB	dB	dB
90	2	-147.29	-29.24	-29.24
90	6	-147.31	-19.68	-19.68
90	10	-147.35	-15.23	-15.23
90	14	-147.41	-12.28	-12.28
90	18	-147.5	-10.07	-10.07
90	22	-147.61	-8.3	-8.3
90	26	-147.76	-6.81	-6.81
90	30	-147.95	-5.54	-5.54
90	34	-148.19	-4.42	-4.42
90	38	-148.48	-3.43	-3.43
90	42	-148.83	-2.55	-2.55
90	46	-149.26	-1.77	-1.77
90	50	-149.78	-1.07	-1.07
90	54	-150.4	-0.44	-0.44
90	58	-151.16	0.11	0.11
90	62	-152.08	0.59	0.59
90	66	-153.2	1.01	1.01
90	70	-154.6	1.36	1.36
90	74	-156.39	1.65	1.65

25×10

90	78	-158.77	1.87	1.87
90	82	-162.2	2.03	2.03
90	86	-168.17	2.13	2.13
90	90	-999.99	2.16	2.16
90	94	-168.17	2.13	2.13
90	98	-162.2	2.03	2.03
90	102	-158.77	1.87	1.87
90	106	-156.39	1.65	1.65
90	110	-154.6	1.36	1.36
90	114	-153.2	1.01	1.01
90	118	-152.08	0.59	0.59
90	122	-151.16	0.11	0.11
90	126	-150.4	-0.44	-0.44
90	130	-149.78	-1.07	-1.07
90	134	-149.26	-1.77	-1.77
90	138	-148.83	-2.55	-2.55
90	142	-148.48	-3.43	-3.43
90	146	-148.19	-4.42	-4.42
90	150	-147.95	-5.54	-5.54
90	154	-147.76	-6.81	-6.81
90	158	-147.61	-8.3	-8.3
90	162	-147.5	-10.07	-10.07
90	166	-147.41	-12.28	-12.28

90	170	-147.35	-15.23	-15.23
90	174	-147.31	-19.68	-19.68
90	178	-147.29	-29.24	-29.24
90	182	-147.29	-29.24	-29.24
90	186	-147.31	-19.68	-19.68
90	190	-147.35	-15.23	-15.23
90	194	-147.41	-12.28	-12.28
90	198	-147.5	-10.07	-10.07
90	202	-147.61	-8.3	-8.3
90	206	-147.76	-6.81	-6.81
90	210	-147.95	-5.54	-5.54
90	214	-148.19	-4.42	-4.42
90	218	-148.48	-3.43	-3.43
90	222	-148.83	-2.55	-2.55
90	226	-149.26	-1.77	-1.77
90	230	-149.78	-1.07	-1.07
90	234	-150.4	-0.44	-0.44
90	238	-151.16	0.11	0.11
90	242	-152.08	0.59	0.59
90	246	-153.2	1.01	1.01
90	250	-154.6	1.36	1.36
90	254	-156.39	1.65	1.65
90	258	-158.77	1.87	1.87

90	262	-162.2	2.03	2.03
90	266	-168.17	2.13	2.13
90	270	-999.99	2.16	2.16
90	274	-168.17	2.13	2.13
90	278	-162.2	2.03	2.03
90	282	-158.77	1.87	1.87
90	286	-156.39	1.65	1.65
90	290	-154.6	1.36	1.36
90	294	-153.2	1.01	1.01
90	298	-152.08	0.59	0.59
90	302	-151.16	0.11	0.11
90	306	-150.4	-0.44	-0.44
90	310	-149.78	-1.07	-1.07
90	314	-149.26	-1.77	-1.77
90	318	-148.83	-2.55	-2.55
90	322	-148.48	-3.43	-3.43
90	326	-148.19	-4.42	-4.42
90	330	-147.95	-5.54	-5.54
90	334	-147.76	-6.81	-6.81
90	338	-147.61	-8.3	-8.3
90	342	-147.5	-10.07	-10.07
90	346	-147.41	-12.28	-12.28
90	350	-147.35	-15.23	-15.23

90	354	-147.31	-19.68	-19.68
90	358	-147.29	-29.24	-29.24
90	362	-147.29	-29.24	-29.24

Zenith-plane radiation pattern of the vertical quarter-wave monopole on a perfectly conducting *infinite ground plane.*

ANGLES		DIRECTIVE GAINS		
Theta	Phi	Vertical	Horizontal	Total
Degrees	Degrees	dB	dB	dB
-90	90	5.16	-999.99	5.16
-88	90	5.15	-999.99	5.15
-86	90	5.13	-999.99	5.13
-84	90	5.09	-999.99	5.09
-82	90	5.03	-999.99	5.03
-80	90	4.96	-999.99	4.96
-78	90	4.87	-999.99	4.87
-76	90	4.77	-999.99	4.77
-74	90	4.65	-999.99	4.65
-72	90	4.51	-999.99	4.51
-70	90	4.36	-999.99	4.36
-68	90	4.19	-999.99	4.19
-66	90	4	-999.99	4
-64	90	3.8	-999.99	3.8
-62	90	3.58	-999.99	3.58
-60	90	3.34	-999.99	3.34
-58	90	3.09	-999.99	3.09
-56	90	2.82	-999.99	2.82
-54	90	2.53	-999.99	2.53

-52	90	2.22	-999.99	2.22
-50	90	1.9	-999.99	1.9
-48	90	1.56	-999.99	1.56
-46	90	1.19	-999.99	1.19
-44	90	0.81	-999.99	0.81
-42	90	0.4	-999.99	0.4
-40	90	-0.03	-999.99	-0.03
-38	90	-0.49	-999.99	-0.49
-36	90	-0.97	-999.99	-0.97
-34	90	-1.48	-999.99	-1.48
-32	90	-2.02	-999.99	-2.02
-30	90	-2.6	-999.99	-2.6
-28	90	-3.22	-999.99	-3.22
-26	90	-3.88	-999.99	-3.88
-24	90	-4.6	-999.99	-4.6
-22	90	-5.37	-999.99	-5.37
-20	90	-6.22	-999.99	-6.22
-18	90	-7.15	-999.99	-7.15
-16	90	-8.19	-999.99	-8.19
-14	90	-9.37	-999.99	-9.37
-12	90	-10.72	-999.99	-10.72
-10	90	-12.32	-999.99	-12.32
-8	90	-14.26	-999.99	-14.26

25×10

-6	90	-16.77	-999.99	-16.77
-4	90	-20.3	-999.99	-20.3
-2	90	-26.32	-999.99	-26.32
0	90	-999.99	-999.99	-999.99
2	90	-26.32	-999.99	-26.32
4	90	-20.3	-999.99	-20.3
6	90	-16.77	-999.99	-16.77
8	90	-14.26	-999.99	-14.26
10	90	-12.32	-999.99	-12.32
12	90	-10.72	-999.99	-10.72
14	90	-9.37	-999.99	-9.37
16	90	-8.19	-999.99	-8.19
18	90	-7.15	-999.99	-7.15
20	90	-6.22	-999.99	-6.22
22	90	-5.37	-999.99	-5.37
24	90	-4.6	-999.99	-4.6
26	90	-3.88	-999.99	-3.88
28	90	-3.22	-999.99	-3.22
30	90	-2.6	-999.99	-2.6
32	90	-2.02	-999.99	-2.02
34	90	-1.48	-999.99	-1.48
36	90	-0.97	-999.99	-0.97
38	90	-0.49	-999.99	-0.49

40	90	-0.03	-999.99	-0.03
42	90	0.4	-999.99	0.4
44	90	0.81	-999.99	0.81
46	90	1.19	-999.99	1.19
48	90	1.56	-999.99	1.56
50	90	1.9	-999.99	1.9
52	90	2.22	-999.99	2.22
54	90	2.53	-999.99	2.53
56	90	2.82	-999.99	2.82
58	90	3.09	-999.99	3.09
60	90	3.34	-999.99	3.34
62	90	3.58	-999.99	3.58
64	90	3.8	-999.99	3.8
66	90	4	-999.99	4
68	90	4.19	-999.99	4.19
70	90	4.36	-999.99	4.36
72	90	4.51	-999.99	4.51
74	90	4.65	-999.99	4.65
76	90	4.77	-999.99	4.77
78	90	4.87	-999.99	4.87
80	90	4.96	-999.99	4.96
82	90	5.03	-999.99	5.03
84	90	5.09	-999.99	5.09

86	90	5.13	-999.99	5.13
88	90	5.15	-999.99	5.15
90	90	5.16	-999.99	5.16

Zenith-plane radiation pattern of the 45° skew quarter-wave monopole on a perfectly conducting infinite ground plane.

ANGLES		DIRECTIVE GAINS		
Theta	Phi	Vertical	Horizontal	Total
Degrees	Degrees	dB	dB	dB
-90	0	4.65	-999.99	4.65
-88	0	4.65	-31.91	4.65
-86	0	4.63	-25.89	4.63
-84	0	4.59	-22.38	4.6
-82	0	4.55	-19.9	4.56
-80	0	4.49	-17.99	4.51
-78	0	4.41	-16.43	4.45
-76	0	4.32	-15.13	4.37
-74	0	4.22	-14	4.29
-72	0	4.11	-13.02	4.19
-70	0	3.98	-12.15	4.08
-68	0	3.84	-11.38	3.97
-66	0	3.68	-10.68	3.84
-64	0	3.51	-10.05	3.7
-62	0	3.32	-9.47	3.55
-60	0	3.12	-8.94	3.38
-58	0	2.9	-8.45	3.21
-56	0	2.67	-8.01	3.03
-54	0	2.42	-7.59	2.83

-52	0	2.15	-7.21	2.63
-50	0	1.87	-6.86	2.42
-48	0	1.57	-6.53	2.19
-46	0	1.24	-6.23	1.96
-44	0	0.9	-5.95	1.72
-42	0	0.54	-5.69	1.47
-40	0	0.15	-5.45	1.21
-38	0	-0.27	-5.22	0.94
-36	0	-0.71	-5.01	0.66
-34	0	-1.18	-4.82	0.38
-32	0	-1.68	-4.64	0.1
-30	0	-2.22	-4.48	-0.2
-28	0	-2.8	-4.33	-0,49
-26	0	-3.43	-4.2	-0.79
-24	0	-4.11	-4.07	-1.08
-22	0	-4.86	-3.96	-1.37
-20	0	-5.67	-3.86	-1.66
-18	0	-6.58	-3.77	-1.94
-16	0	-7.6	-3.69	-2.2
-14	0	-8.75	-3.62	-2.45
-12	0	-10.08	-3.55	-2.68
-10	0	-11.66	-3.5	-2.89
-8	0	-13.6	-3.46	-3.06

-6	0	-16.09	-3.43	-3.2
-4	0	-19.61	-3.41	-3.31
-2	0	-25.63	-3.39	-3.37
0	0	-999.99	-3.39	-3.39
2	0	-25.63	-3.39	-3.37
4	0	-19.61	-3.41	-3.31
6	0	-16.09	-3.43	-3.2
8	0	-13.6	-3.46	-3.06
10	0	-11.66	-3.5	-2.89
12	0	-10.08	-3.55	-2.68
14	0	-8.75	-3.62	-2.45
16	0	-7.6	-3.69	-2.2
18	0	-6.58	-3.77	-1.94
20	0	-5.67	-3.86	-1.66
22	0	-4.86	-3.96	-1.37
24	0	-4.11	-4.07	-1.08
26	0	-3.43	-4.2	-0.79
28	0	-2.8	-4.33	-0.49
30	0	-2.22	-4.48	-0.2
32	0	-1.68	-4.64	0.1
34	0	-1.18	-4.82	0.38
36	0	-0.71	-5.01	0.66
38	0	-0.27	-5.22	0.94

40	0	0.15	-5.45	1.21
42	0	0.54	-5.69	1.47
44	0	0.9	-5.95	1.72
46	0	1.24	-6.23	1.96
48	0	1.57	-6.53	2.19
50	0	1.87	-6.86	2.42
52	0	2.15	-7.21	2.63
54	0	2.42	-7.59	2.83
56	0	2.67	-8.01	3.03
58	0	2.9	-8.45	3.21
60	0	3.12	-8.94	3.38
62	0	3.32	-9.47	3.55
64	0	3.51	-10.05	3.7
66	0	3.68	-10.68	3.84
68	0	3.84	-11.38	3.97
70	0	3.98	-12.15	4.08
72	0	4.11	-13.02	4.19
74	0	4.22	-14	4.29
76	0	4.32	-15.13	4.37
78	0	4.41	-16.43	4.45
80	0	4.49	-17.99	4.51
82	0	4.55	-19.9	4.56
84	0	4.59	-22.38	4.6

86	0	4.63	-25.89	4.63
88	0	4.65	-31.91	4.65

Azimuth-plane radiation pattern of the 45° skew quarter-wave monopole on a perfectly conducting infinite ground plane.

ANGLES		DIRECTIVE GAINS		
Theta	Phi	Vertical	Horizontal	Total
Degrees	Degrees	dB	dB	dB
90	0	4.65	-999.99	4.65
90	2	4.65	-999.99	4.65
90	4	4.65	-999.99	4.65
90	6	4.65	-999.99	4.65
90	8	4.65	-141.98	4.65
90	10	4.65	-999.99	4.65
90	12	4.64	-145.1	4.64
90	14	4.64	-999.99	4.64
90	16	4.63	-999.99	4.63
90	18	4.63	-145.34	4.63
90	20	4.62	-138.46	4.62
90	22	4.62	-999.99	4.62
90	24	4.61	-999.99	4.61
90	26	4.6	-999.99	4.6
90	28	4.59	-999.99	4.59
90	30	4.58	-999.99	4.58
90	32	4.57	-146.34	4.57
90	34	4.56	-999.99	4.56
90	36	4.55	-146.75	4.55

90	38	4.54	-999.99	4.54
90	40	4.53	-153.24	4.53
90	42	4.52	-153.51	4.52
90	44	4.51	-141.75	4.51
90	46	4.5	-154.09	4.5
90	48	4.49	-154.42	4.49
90	50	4.48	-148.74	4.48
90	52	4.47	-149.12	4.47
90	54	4.46	-148.55	4.46
90	56	4.45	-999.99	4.45
90	58	4.44	-156.44	4.44
90	60	4.43	-150.93	4.43
90	62	4.42	-151.47	4.42
90	64	4.41	-148.55	4.41
90	66	4.4	-158.74	4.4
90	68	4.39	-159.46	4.39
90	70	4.38	-154.23	4.38
90	72	4.38	-151.58	4.38
90	74	4.37	-153.09	4.37
90	76	4.36	-163.25	4.36
90	78	4.36	-999.99	4.36
90	80	4.36	-160.11	4.36
90	82	4.35	-162.04	4.35

90	84	4.35	-999.99	4.35
90	86	4.35	-174.06	4.35
90	88	4.35	-180.07	4.35
90	90	4.35	-999.99	4.35
90	92	4.35	-180.07	4.35
90	94	4.35	-174.06	4.35
90	96	4.35	-999.99	4.35
90	98	4.35	-162.04	4.35
90	100	4.36	-160.11	4.36
90	102	4.36	-999.99	4.36
90	104	4.36	-163.25	4.36
90	106	4.37	-153.09	4.37
90	108	4.38	-151.58	4.38
90	110	4.38	-154.23	4.38
90	112	4.39	-159.46	4.39
90	114	4.4	-158.74	4.4
90	116	4.41	-148.55	4.41
90	118	4.42	-151.47	4.42
90	120	4.43	-147.92	4.43
90	122	4.44	-156.44	4.44
90	124	4.45	-155.98	4.45
90	126	4.46	-148.55	4.46
90	128	4.47	-149.12	4.47

90	130	4.48	-148.74	4.48
90	132	4.49	-999.99	4.49
90	134	4.5	-148.07	4.5
90	136	4.51	-146.8	4.51
90	138	4.52	-153.51	4.52
90	140	4.53	-147.22	4.53
90	142	4.54	-999.99	4.54
90	144	4.55	-146.75	4.55
90	146	4.56	-999.99	4.56
90	148	4.57	-146.34	4.57
90	150	4.58	-146.16	4.58
90	152	4.59	-999.99	4.59
90	154	4.6	-999.99	4.6
90	156	4.61	-139.67	4.61
90	158	4.62	-999.99	4.62
90	160	4.62	-145.45	4.62
90	162	4.63	-139.32	4.63
90	164	4.63	-999.99	4.63
90	166	4.64	-999.99	4.64
90	168	4.64	-145.1	4.64
90	170	4.65	-142.03	4.65
90	172	4.65	-141.98	4.65
90	174	4.65	-999.99	4.65

90	176	4.65	-999.99	4.65
90	178	4.65	-144.91	4.65
90	180	4.65	-999.99	4.65
90	182	4.65	-999.99	4.65
90	184	4.65	-144.93	4.65
90	186	4.65	-144.95	4.65
90	188	4.64	-144.99	4.64
90	190	4.64	-145.04	4.64
90	192	4.63	-139.08	4.63
90	194	4.63	-999.99	4.63
90	196	4.62	-999.99	4.62
90	198	4.61	-999.99	4.61
90	200	4.6	-144.48	4.6
90	202	4.59	-151.58	4.59
90	204	4.58	-142.68	4.58
90	206	4.57	-145.83	4.57
90	208	4.56	-152.01	4.56
90	210	4.55	-152.18	4.55
90	212	4.54	-999.99	4.54
90	214	4.53	-146.53	4.53
90	216	4.52	-152.77	4.52
90	218	4.51	-153	4.51
90	220	4.49	-147.22	4.49

90	222	4.48	-147.48	4.48
90	224	4.47	-153.79	4.47
90	226	4.46	-145.06	4.46
90	228	4.44	-999.99	4.44
90	230	4.43	-148.74	4.43
90	232	4.42	-999.99	4.42
90	234	4.41	-999.99	4.41
90	236	4.4	-155.98	4.4
90	238	4.39	-149.45	4.39
90	240	4.37	-156.95	4.37
90	242	4.36	-148.46	4.36
90	244	4.35	-152.07	4.35
90	246	4.34	-158.74	4.34
90	248	4.34	-153.43	4.34
90	250	4.33	-154.23	4.33
90	252	4.32	-999.99	4.32
90	254	4.31	-162.12	4.31
90	256	4.31	-999.99	4.31
90	258	4.3	-158.55	4.3
90	260	4.3	-999.99	4.3
90	262	4.29	-168.06	4.29
90	264	4.29	-170.54	4.29
90	266	4.29	-167.07	4.29

90	268	4.29	-171.04	4.29
90	270	4.29	-999.99	4.29
90	272	4.29	-171.04	4.29
90	274	4.29	-167.07	4.29
90	276	4.29	-170.54	4.29
90	278	4.29	-168.06	4.29
90	280	4.3	-159.14	4.3
90	282	4.3	-158.55	4.3
90	284	4.31	-999.99	4.31
90	286	4.31	-162.12	4.31
90	288	4.32	-999.99	4.32
90	290	4.33	-999.99	4.33
90	292	4.34	-999.99	4.34
90	294	4.34	-158.74	4.34
90	296	4.35	-152.07	4.35
90	298	4.36	-148.46	4.36
90	300	4.37	-156.95	4.37
90	302	4.39	-150.42	4.39
90	304	4.4	-155.98	4.4
90	306	4.41	-999.99	4.41
90	308	4.42	-999.99	4.42
90	310	4.43	-999.99	4.43
90	312	4.44	-999.99	4.44

90	314	4.46	-145.06	4.46
90	316	4.47	-147.77	4.47
90	318	4.48	-146.52	4.48
90	320	4.49	-147.22	4.49
90	322	4.51	-153	4.51
90	324	4.52	-140.73	4.52
90	326	4.53	-146.53	4.53
90	328	4.54	-999.99	4.54
90	330	4.55	-152.18	4.55
90	332	4.56	-145.99	4.56
90	334	4.57	-151.85	4.57
90	336	4.58	-151.71	4.58
90	338	4.59	-151.58	4.59
90	340	4.6	-999.99	4.6
90	342	4.61	-145.34	4.61
90	344	4.62	-999.99	4.62
90	346	4.63	-145.17	4.63
90	348	4.63	-142.09	4.63
90	350	4.64	-999.99	4.64
90	352	4.64	-144.99	4.64
90	354	4.65	-144.95	4.65
90	356	4.65	-144.93	4.65
90	358	4.65	-999.99	4.65

Zenith-plane radiation pattern of the square loop antenna.

ANGLES		DIRECTIVE GAINS		
Theta	Phi	Vertical	*Horizontal*	Total
Degrees	*Degrees*	dB	dB	dB
-90	90	-999.99	-999.99	-999.99
-89	90	-76.77	-28.78	-28.78
-88	90	-64.73	-22.75	-22.75
-87	90	-57.69	-19.23	-19.23
-86	90	-52.69	-16.73	-16.73
-85	90	-48.82	-14.78	-14.78
-84	90	-45.66	-13.19	-13.19
-83	90	-43	-11.85	-11.84
-82	90	-40.69	-10.68	-10.68
-81	90	-38.65	-9.65	-9.64
-80	90	-36.83	-8.72	-8.71
-79	90	-35.19	-7.88	-7.87
-78	90	-33.69	-7.11	-7.1
-77	90	-32.32	-6.41	-6.39
-76	90	-31.05	-5.75	-5.73
-75	90	-29.87	-5.13	-5.12
-74	90	-28.77	-4.56	-4.54
-73	90	-27.74	-4.01	-4
-72	90	-26.77	-3.5	-3.48

-71	90	-25.86	-3.01	-2.99
-70	90	-24.99	-2.55	-2.53
-69	90	-24.17	-2.11	-2.08
-68	90	-23.39	-1.68	-1.65
-67	90	-22.65	-1.28	-1.25
-66	90	-21.95	-0.89	-0.85
-65	90	-21.27	-0.51	-0.48
-64	90	-20.63	-0.15	-0.11
-63	90	-20.01	0.19	0.24
-62	90	-19.41	0.53	0.57
-61	90	-18.85	0.86	0.9
-60	90	-18.3	1.17	1.22
-59	90	-17.77	1.48	1.53
-58	90	-17.27	1.77	1.83
-57	90	-16.78	2.06	2.11
-56	90	-16.31	2.34	2.4
-55	90	-15.86	2.61	2.67
-54	90	-15.42	2.87	2.93
-53	90	-15	3.13	3.19
-52	90	-14.59	3.37	3.44
-51	90	-14.2	3.62	3.69
-50	90	-13.82	3.85	3.92
-49	90	-13.45	4.08	4.16

-48	90	-13.09	4.3	4.38
-47	90	-12.75	4.52	4.6
-46	90	-12.42	4.73	4.81
-45	90	-12.1	4.94	5.02
-44	90	-11.79	5.14	5.22
-43	90	-11.49	5.33	5.42
-42	90	-11.19	5.52	5.61
-41	90	-10.91	5.7	5.8
-40	90	-10.64	5.88	5.98
-39	90	-10.38	6.06	6.15
-38	90	-10.13	6.23	6.33
-37	90	-9.88	6.39	6.49
-36	90	-9.65	6.55	6.65
-35	90	-9.42	6.7	6.81
-34	90	-9.2	6.85	6.96
-33	90	-8.99	7	7.11
-32	90	-8.78	7.14	7.25
-31	90	-8.58	7.28	7.39
-30	90	-8.39	7.41	7.52
-29	90	-8.21	7.54	7.65
-28	90	-8.04	7.66	7.77
-27	90	-7.87	7.78	7.89
-26	90	-7.71	7.89	8.01

25X1

-25	90	-7.55	8	8.12
-24	90	-7.41	8.1	8.22
-23	90	-7.27	8.2	8.33
-22	90	-7.13	8.3	8.42
-21	90	-7	8.39	8.52
-20	90	-6.88	8.48	8.61
-19	90	-6.77	8.56	8.69
-18	90	-6.66	8.64	8.77
-17	90	-6.56	8.72	8.84
-16	90	-6.46	8.79	8.92
-15	90	-6.37	8.85	8.98
-14	90	-6.29	8.92	9.05
-13	90	-6.21	8.97	9.1
-12	90	-6.14	9.03	9.16
-11	90	-6.07	9.08	9.21
-10	90	-6.01	9.12	9.25
-9	90	-5.95	9.16	9.29
-8	90	-5.91	9.2	9.33
-7	90	-5.86	9.23	9.36
-6	90	-5.83	9.26	9.39
-5	90	-5.79	9.28	9.42
-4	90	-5.77	9.3	9.44
-3	90	-5.75	9.32	9.45

-2	90	-5.74	9.33	9.46
-1	90	-5.73	9.34	9.47
0	90	-5.72	9.34	9.47
1	90	-5.73	9.34	9.47
2	90	-5.74	9.33	9.46
3	90	-5.75	9.32	9.45
4	90	-5.77	9.31	9.44
5	90	-5.8	9.29	9.42
6	90	-5.83	9.27	9.4
7	90	-5.87	9.24	9.37
8	90	-5.91	9.21	9.34
9	90	-5.96	9.17	9.3
10	90	-6.02	9.13	9.26
11	90	-6.08	9.09	9.22
12	90	-6.14	9.04	9.17
13	90	-6.22	8.99	9.12
14	90	-6.3	8.93	9.06
15	90	-6.38	8.87	9
16	90	-6.47	8.81	8.93
17	90	-6.57	8.74	8.86
18	90	-6.67	8.67	8.79
19	90	-6.78	8.59	8.71
20	90	-6.9	8.51	8.63

21	90	-7.02	8.42	8.54
22	90	-7.15	8.33	8.45
23	90	-7.28	8.23	8.35
24	90	-7.42	8.13	8.25
25	90	-7.57	8.03	8.15
26	90	-7.73	7.92	8.04
27	90	-7.89	7.81	7.92
28	90	-8.06	7.69	7.81
29	90	-8.23	7.57	7.68
30	90	-8.41	7.45	7.56
31	90	-8.6	7.32	7.42
32	90	-8.8	7.18	7.29
33	90	-9.01	7.04	7.15
34	90	-9.22	6.9	7
35	90	-9.44	6.75	6.85
36	90	-9.67	6.59	6.7
37	90	-9.91	6.44	6.54
38	90	-10.15	6.27	6.37
39	90	-10.41	6.11	6.2
40	90	-10.67	5.93	6.03
41	90	-10.94	5.75	5.85
42	90	-11.22	5.57	5.66
43	90	-11.51	5.38	5.47

44	90	-11.81	5.19	5.28
45	90	-12.12	4.99	5.08
46	90	-12.45	4.79	4.87
47	90	-12.78	4.58	4.66
48	90	-13.12	4.36	4.44
49	90	-13.48	4.14	4.21
50	90	-13.85	3.91	3.98
51	90	-14.23	3.68	3.75
52	90	-14.62	3.44	3.51
53	90	-15.03	3.19	3.26
54	90	-15.45	2.94	3
55	90	-15.89	2.67	2.73
56	90	-16.34	2.41	2.46
57	90	-16.81	2.13	2.18
58	90	-17.3	1.84	1.89
59	90	-17.81	1.55	1.6
60	90	-18.33	1.24	1.29
61	90	-18.88	0.93	0.98
62	90	-19.45	0.61	0.65
63	90	-20.04	0.27	0.31
64	90	-20.66	-0.08	-0.04
65	90	-21.31	-0.44	-0.4
66	90	-21.98	-0.81	-0.78

67	90	-22.69	-1.2	-1.17
68	90	-23.43	-1.6	-1.58
69	90	-24.21	-2.03	-2
70	90	-25.03	-2.47	-2.44
71	90	-25.9	-2.93	-2.91
72	90	-26.81	-3.42	-3.4
73	90	-27.78	-3.93	-3.91
74	90	-28.81	-4.47	-4.46
75	90	-29.91	-5.05	-5.03
76	90	-31.09	-5.66	-5.65
77	90	-32.36	-6.32	-6.31
78	90	-33.73	-7.03	-7.02
79	90	-35.23	-7.8	-7.79
80	90	-36.87	-8.63	-8.63
81	90	-38.69	-9.56	-9.55
82	90	-40.72	-10.59	-10.59
83	90	-43.03	-11.76	-11.76
84	90	-45.7	-13.11	-13.1
85	90	-48.86	-14.69	-14.69
86	90	-52.73	-16.64	-16.64
87	90	-57.73	-19.14	-19.14
88	90	-64.77	-22.67	-22.66
89	90	-76.81	-28.69	-28.69

Azimuth-plane radiation pattern of the *square* loop antenna sliced at zenith angle $\theta = 70°$.

ANGLES		DIRECTIVE GAINS		
Theta	*Phi*	Vertical	Horizontal	Total
Degrees	Degrees	dB	dB	dB
70	0	-9.94	-16.46	-9.07
70	2	-10	-15.08	-8.83
70	4	-10.07	-13.88	-8.56
70	6	-10.15	-12.82	-8.28
70	8	-10.25	-11.88	-7.98
70	10	-10.36	-11.04	-7.68
70	12	-10.48	-10.28	-7.37
70	14	-10.61	-9.59	-7.06
70	16	-10.76	-8.96	-6.76
70	18	-10.92	-8.38	-6.46
70	20	-11.1	-7.85	-6.17
70	22	-11.29	-7.36	-5.89
70	24	-11.5	-6.91	-5.62
70	26	-11.73	-6.5	-5.36
70	28	-11.97	-6.11	-5.11
70	30	-12.23	-5.75	-4.87
70	32	-12.5	-5.42	-4.64
70	34	-12.8	-5.11	-4.43
70	36	-13.12	-4.82	-4.22

70	38	-13.46	-4.56	-4.03
70	40	-13.83	-4.31	-3.85
70	42	-14.22	-4.08	-3.68
70	44	-14.65	-3.87	-3.52
70	46	-15.1	-3.68	-3.37
70	48	-15.59	-3.5	-3.24
70	50	-16.12	-3.33	-3.11
70	52	-16.69	-3.18	-2.99
70	54	-17.31	-3.05	-2.89
70	56	-17.99.	-2.92	-2.79
70	58	-18.73	-2.81	-2.7
70	60	-19.56	-2.71	-2.62
70	62	-20.47	-2.63	-2.55
70	64	-21.51	-2.55	-2.49
70	66	-22.69	-2.48	-2.44
70	68	-24.07	-2.43	-2.4
70	70	-25.71	-2.38	-2.36
70	72	-27.75	-2.35	-2.34
70	74	-30.42	-2.33	-2.32
70	76	-34.29	-2.31	-2.31
70	78	-41.43	-2.31	-2.3
70	80	-51.67	-2.31	-2.31
70	82	-37.55	-2.32	-2.32

70	84	-32.39	-2.35	-2.34
70	86	-29.18	-2.38	-2.37
70	88	-26.86	-2.42	-2.4
70	90	-25.03	-2.47	-2.44
70	92	-23.53	-2.53	-2.49
70	94	-22.26	-2.6	-2.55
70	96	-21.17	-2.68	-2.61
70	98	-20.2	-2.76	-2.69
70	100	-19.34	-2.86	-2.77
70	102	-18.57	-2.97	-2.85
70	104	-17.86	-3.09	-2.95
70	106	-17.22	-3.22	-3.05
70	108	[illegible]	-3.36	-3.16
70	110	-16.09	-3.52	-3.28
70	112	-15.59	-3.68	-3.41
70	114	-15.12	-3.86	-3.55
70	116	-14.69	-4.05	-3.69
70	118	-14.28	-4.26	-3.85
70	120	-13.9	-4.48	-4.01
70	122	-13.55	-4.72	-4.19
70	124	-13.22	-4.98	-4.37
70	126	-12.9	-5.25	-4.57
70	128	-12.61	-5.55	-4.77

70	130	-12.34	-5.87	-4.98
70	132	-12.09	-6.21	-5.21
70	134	-11.85	-6.57	-5.44
70	136	-11.62	-6.96	-5.69
70	138	-11.42	-7.39	-5.94
70	140	-11.22	-7.85	-6.2
70	142	-11.04	-8.34	-6.48
70	144	-10.88	-8.88	-6.76
70	146	-10.72	-9.47	-7.04
70	148	-10.58	-10.11	-7.33
70	150	-10.46	-10.82	-7.62
70	152	-10.34	-11.6	-7.91
70	154	-10.24	-12.47	-8.2
70	156	-10.14	-13.44	-8.48
70	158	-10.06	-14.54	-8.74
70	160	-9.99	-15.81	-8.98
70	162	-9.94	-17.27	-9.2
70	164	-9.89	-18.97	-9.38
70	166	-9.86	-20.94	-9.53
70	168	-9.83	-23.08	-9.63
70	170	-9.82	-24.78	-9.68
70	172	-9.82	-24.85	-9.68
70	174	-9.83	-23.2	-9.63

70	176	-9.85	-21.05	-9.53
70	178	-9.88	-19.04	-9.39
70	180	-9.93	-17.3	-9.2
70	182	-9.99	-15.8	-8.97
70	184	-10.05	-14.51	-8.72
70	186	-10.13	-13.38	-8.45
70	188	-10.23	-12.38	-8.16
70	190	-10.33	-11.49	-7.86
70	192	-10.45	-10.69	-7.56
70	194	-10.58	-9.96	-7.25
70	196	-10.73	-9.3	-6.95
70	198	-10.89	-8.7	-6.65
70	200	-11.06	-8.14	-6.35
70	202	-11.25	-7.63	-6.07
70	204	-11.46	-7.16	-5.79
70	206	-11.68	-6.73	-5.52
70	208	-11.92	-6.33	-5.27
70	210	-12.17	-5.96	-5.03
70	212	-12.45	-5.61	-4.79
70	214	-12.74	-5.29	-4.57
70	216	-13.06	-4.99	-4.36
70	218	-13.4	-4.72	-4.17
70	220	-13.77	-4.46	-3.98

70	222	-14.16	-4.23	-3.81
70	224	-14.58	-4.01	-3.64
70	226	-15.03	-3.81	-3.49
70	228	-15.51	-3.62	-3.35
70	230	-16.04	-3.45	-3.22
70	232	-16.61	-3.3	-3.1
70	234	-17.23	-3.16	-2.99
70	236	-17.9	-3.03	-2.89
70	238	-18.64	-2.91	-2.8
70	240	-19.46	-2.81	-2.72
70	242	-20.38	-2.72	-2.65
70	244	-21.41	-2.64	-2.58
70	246	-22.59	-2.57	-2.53
70	248	-23.96	-2.52	-2.49
70	250	-25.59	-2.47	-2.45
70	252	-27.62	-2.43	-2.42
70	254	-30.26	-2.41	-2.4
70	256	-34.09	-2.39	-2.39
70	258	-41.09	-2.39	-2.38
70	260	-52.43	-2.39	-2.39
70	262	-37.65	-2.4	-2.4
70	264	-32.41	-2.42	-2.42
70	266	-29.17	-2.46	-2.45

70	268	-26.83	-2.5	-2.48
70	270	-24.99	-2.55	-2.53
70	272	-23.49	-2.61	-2.58
70	274	-22.22	-2.68	-2.63
70	276	-21.12	-2.76	-2.7
70	278	-20.15	-2.85	-2.77
70	280	-19.29	-2.95	-2.85
70	282	-18.51	-3.07	-2.94
70	284	-17.81	-3.19	-3.04
70	286	-17.17	-3.32	-3.15
70	288	-16.58	-3.47	-3.26
70	290	-16.03	-3.63	-3.39
70	292	-15.53	-3.8	-3.52
70	294	-15.06	-3.98	-3.66
70	296	-14.63	-4.18	-3.81
70	298	-14.22	-4.4	-3.97
70	300	-13.85	-4.63	-4.14
70	302	-13.49	-4.87	-4.31
70	304	-13.16	-5.14	-4.5
70	306	-12.85	-5.42	-4.7
70	308	-12.56	-5.73	-4.91
70	310	-12.29	-6.06	-5.13
70	312	-12.04	-6.41	-5.36

70	314	-11.8	-6.79	-5.6
70	316	-11.58	-7.2	-5.85
70	318	-11.38	-7.64	-6.11
70	320	-11.18	-8.12	-6.37
70	322	-11.01	-8.63	-6.65
70	324	-10.84	-9.2	-6.93
70	326	-10.69	-9.81	-7.22
70	328	-10.55	-10.49	-7.51
70	330	-10.43	-11.23	-7.8
70	332	-10.32	-12.06	-8.09
70	334	-10.21	-12.98	-8.37
70	336	-10.12	-14.02	-8.64
70	338	-10.05	-15.2	-8.89
70	340	-9.98	-16.57	-9.12
70	342	-9.93	-18.15	-9.32
70	344	-9.89	-20	-9.48
70	346	-9.85	-22.09	-9.6
70	348	-9.83	-24.12	-9.67
70	350	-9.82	-25.08	-9.69
70	352	-9.82	-24.09	-9.66
70	354	-9.83	-22.04	-9.58
70	356	-9.86	-19.94	-9.45
70	358	-9.89	-18.07	-9.28

Azimuth-plane radiation pattern of the long wire (terminated) antenna sliced at zenith angle θ = 80°.

ANGLES		DIRECTIVE GAINS		
Theta	Phi	Vertical	Horizontal	Total
Degrees	Degrees	dB	dB	dB
80	0	-999.99	-6	-6
80	4	-49.69	-11.38	-11.38
80	8	-35.68	-3.43	-3.42
80	12	-32.57	-3.91	-3.9
80	16	-37.2[illegible]	-11.72	-11.71
80	20	-26	-2.01	-1.99
80	24	-29.83	-7.59	-7.5[illegible]
80	28	-23.17	-2.47	-2.44
80	32	-26.71	-7.42	-7.36
80	36	-18.72	-0.74	-0.67
80	40	-25.48	-8.75	-8.66
80	44	-21.7	-6.[illegible]	-6.07
80	48	-14.94	-0.64	-0.49
80	52	-12.22	0.84	1.05
80	56	-10.36	1.44	1.72
80	60	-9.33	1.1	1.48
80	64	-13.42	-4.45	-3.93
80	68	-9.27	-1.93	-1.19
80	72	-0.9	4.54	5.63

80	76	-6.58	-3.44	-1.72
80	80	2.75	2.88	5.82
80	84	9.26	4.9	10.61
80	88	11.13	-2.8	11.3
80	92	11.13	-2.8	11.3
80	96	9.26	4.9	10.61
80	100	2.75	2.88	5.82
80	104	-6.58	-3.44	-1.72
80	108	-0.9	4.54	5.63
80	112	-9.27	-1.93	-1.19
80	116	-13.42	-4.45	-3.93
80	120	-9.33	1.1	1.48
80	124	-10.35	1.44	1.72
80	128	-12.22	0.84	1.05
80	132	-14.94	-0.64	-0.49
80	136	-21.7	-6.19	-6.07
80	140	-25.48	-8.75	-8.66
80	144	-18.72	-0.74	-0.67
80	148	-26.71	-7.42	-7.36
80	152	-23.17	-2.47	-2.44
80	156	29.83	-7.59	-7.57
80	160	-26	-2.01	-1.99
80	164	-37.78	-11.72	-11.71

80	168	-32.57	-3.91	-3.9
80	172	-35.68	-3.43	-3.42
80	176	-49.69	-11.38	-11.38
80	180	-162.38	-6	-6
80	184	-42.22	-3.91	-3.91
80	188	-41.56	-9.31	-9.3
80	192	-37.47	-8.81	-8.8
80	196	-31.26	-5.21	-5.19
80	200	-35.91	-11.93	-11.91
80	204	-29.74	-7.51	-7.48
80	208	-30.44	-9.75	-9.71
80	212	-28.37	-9.08	-9.03
80	216	-31.41	-13.43	-13.36
80	220	-25.31	-8.58	-8.49
80	224	-28.18	-12.67	-12.55
80	228	-35.88	-21.59	-21.43
80	232	-30.84	-17.77	-17.56
80	236	-28.33	-16.54	-16.26
80	240	-30.69	-20.26	-19.88
80	244	-34.78	-25.81	-25.29
80	248	-18.39	-11.06	-10.32
80	252	-15.6	-10.16	-9.07
80	256	-15.97	-12.83	-11.11

80	260	-11.86	-11.72	-8.78
80	264	-3.78	-8.15	-2.43
80	268	-1.55	-15.49	-1.38
80	272	-1.55	-15.49	-1.38
80	276	-3.78	-8.15	-2.43
80	280	-11.86	-11.72	-8.78
80	284	-15.97	-12.83	-11.11
80	288	-15.6	-10.16	-9.07
80	292	-18.39	-11.06	-10.32
80	296	-34.78	-25.81	-25.29
80	300	-30.69	-20.26	-19.88
80	304	-28.33	-16.54	-16.26
80	308	-30.84	-17.77	-17.56
80	312	-35.88	-21.59	-21.43
80	316	-28.18	-12.67	-12.55
80	320	-25.32	-8.58	-8.49
80	324	-31.41	-13.43	-13.36
80	328	-28.37	-9.08	-9.03
80	332	-30.44	-9.75	-9.71
80	336	-29.74	-7.51	-7.48
80	340	-35.91	-11.93	-11.91
80	344	-31.26	-5.21	-5.19
80	348	-37.47	-8.81	-8.8

80	352	-41.56	-9.31	-9.3
80	356	-42.22	-3.91	-3.91

Zenith-plane radiation pattern of the long wire (terminated) antenna.

ANGLES		DIRECTIVE GAINS		
Theta	Phi	Vertical	Horizontal	Total
Degrees	Degrees	dB	dB	dB
-90	90	-999.99	-999.99	-999.99
-88	90	-26.27	-144.32	-26.27
-86	90	-14.36	-138.42	-14.36
-84	90	-7.69	-135.26	-7.69
-82	90	-3.52	-133.58	-3.52
-80	90	-1.33	-133.31	-1.33
-78	90	-1.41	-134.96	-1.41
-76	90	-5.58	-140.44	-5.58
-74	90	-19.79	-155.78	-19.79
-72	90	-3.52	-140.5	-3.52
-70	90	-2.42	-140.29	-2.42
-68	90	-15.93	-154.59	-15.93
-66	90	-4.02	-143.39	-4.02
-64	90	-3.93	-143.95	-3.93
-62	90	-11.64	-152.26	-11.64
-60	90	-2.27	-143.44	-2.27
-58	90	-22.72	-164.39	-22.72
-56	90	-1.82	-143.96	-1.82
-54	90	-17.06	-159.63	-17.06

-52	90	-1.54	-144.51	-1.54
-50	90	-7.98	-151.33	-7.98
-48	90	-2.8	-146.5	-2.8
-46	90	-1.78	-145.81	-1.78
-44	90	-9.73	-154.06	-9.73
-42	90	-0.23	-144.84	-0.23
-40	90	-2.04	-146.92	-2.04
-38	90	-7.47	-152.59	-7.47
-36	90	0.16	-145.19	0.16
-34	90	0.34	-145.22	0.34
-32	90	-5.41	-151.17	-5.41
-30	90	-2.9	-148.84	-2.9
-28	90	1.43	-144.67	1.43
-26	90	1.4	-144.86	1.4
-24	90	-2.29	-148.69	-2.29
-22	90	-5.3	-151.83	-5.3
-20	90	-0.27	-146.92	-0.27
-18	90	2.41	-144.34	2.41
-16	90	2.65	-144.2	2.65
-14	90	0.78	-146.15	0.78
-12	90	-3.15	-150.14	-3.15
-10	90	-4.28	-151.34	-4.28
-8	90	-0.05	-147.16	-0.05

-6	90	2.77	-144.37	2.77
-4	90	3.89	-143.27	3.89
-2	90	3.57	-143.61	3.57
0	90	1.71	-145.47	1.71
2	90	-2.03	-149.21	-2.03
4	90	-4.24	-151.4	-4.24
6	90	0.26	-146.88	0.26
8	90	3.73	-143.38	3.73
10	90	5.26	-141.79	5.26
12	90	5.03	-141.97	5.03
14	90	2.56	-144.36	2.56
16	90	-3.19	-150.03	-3.19
18	90	-0.66	-147.42	-0.66
20	90	4.86	-141.79	4.86
22	90	6.73	-139.8	6.73
24	90	5.23	-141.18	5.23
26	90	-2.03	-148.29	-2.03
28	90	1.59	-144.51	1.59
30	90	7.27	-138.67	7.27
32	90	6.85	-138.9	6.85
34	90	-2.71	-148.27	-2.71
36	90	4.97	-140.38	4.97
38	90	8.55	-136.56	8.55

40	90	1.55	-143.32	1.55
42	90	5.2	-139.41	5.2
44	90	8.96	-135.36	8.96
46	90	-6.34	-150.36	-6.34
48	90	9.1	-134.6	9.1
50	90	4.72	-138.63	4.72
52	90	7.67	-135.3	7.67
54	90	7.22	-135.36	7.22
56	90	7.6	-134.54	7.6
58	90	6.58	-135.09	6.58
60	90	9.59	-131.58	9.59
62	90	-0.68	-141.3	-0.68
64	90	11.04	-128.99	11.04
66	90	4.8	-134.57	4.8
68	90	6	-132.66	6
70	90	11.46	-126.41	11.46
72	90	7.84	-129.14	7.84
74	90	-8.22	-144.21	-8.22
76	90	8.89	-125.97	8.89
78	90	11.75	-121.8	11.75
80	90	11.32	-120.66	11.32
82	90	8.85	-121.21	8.85
84	90	4.53	-123.04	4.53

86	90	-2.23	-126.29	-2.23
88	90	-14.19	-132.23	-14.19

RFERENCES

[1]. Ince, AN. "*Communications Through EM-Wave Scattering*" IEEE Communications Magazine, Vol 20, No 3, May 1982, pp 27-43.

[2]. Day, WE. "Meteor Burst Communications Bounce Signals Between Remote Sites" Electronics, Vol 55, No 26, Dec. 1982, pp71-75.

[3]. Westwater, GE. "Meteor Burst Communications Systems" Pacific Telecommunications Council (PTC), Honalulu Hi, USA, Jan. 1983.

[4]. Oetting, JD. "An Analysis of Meteor Burst Communications for Military Applications" IEEE Transactions on Communications, Vol COM-28, No 9 Pt1, Sept. 1980, pp 1591-1601.

[5]. Gottlieb, I. "*Meteoric Burst Could Keep Post-Attack Communication Open*" *Defence* Electronics, Vol 13, No 11, USA, Nov. 1981, pp 61-69.

[6]. Richmond, RL. "Meteor Burst Communications Part I: MBC Advances Assist C3 Objectives" Military Electronics/Countermeasures (USA), Vol 8, No 8, August 1982, pp 68-72.

[7]. Herman, JR.; Duggan, CC.; Thompson, WL; Costa, RA. and Deluca, DM. "Narrowband Digital Voice Communications Over A Meteor Burst Channel" Electron. Lett. (GB) Vol. 23, No. 1, 2 Jan. 1987, [illegible].

[8]. Hines, CO.; Forsyth, PA.; Vogan, EL. and Pug[illegible] "T[illegible] ependence of Meteoric *Forward-Scattering* on Antenna Patterns and O[illegible] Can. J. Phys., Vol. 33, 1955, pp. 609-610.

[9]. Hines, CO. and O'grady, M. "Height-Gain in the Forward-Scattering of Radio Waves by Meteor Trails" Can. J.,Phys. Vol. 35, 1957, pp. 125-127.

[10]. Harrington, RF. "Field Computation by Moment Methods" Macmillan, New York, 1968.

[11]. Stutzman, WL. and Thiele, GA. "Antenna Theory and Design" Chapters 2 & 6, John Wiley and Sons, Inc. 1981.

[12]. Burke, GJ. and Poggio, AJ. "Numerical Electromagnetic Code (NEC) - Method of Moments" Parts I, II, III. NOSC Tech Doc 116, Naval Ocean Systems Centre, San Diego, CA., Jully 1977 (NEC1); Revised Jan. 1980 (NEC2).

[13]. Larsen, JL. and Rodman, PJ. "Study Into Meteor Scatter Communication Systems, Project IV Part 2, Computer Prediction Model" SALBU (PTY)Ltd. Internal Report, 1987.

[14]. Ludlow, JDV. "VHF Meteor Scatter Propagation" Radio Communication (GB), Vol 51, No 2, Feb. 1975, pp 100-107.

[15]. Sugar, RG. "Radio Propagation by Reflection from Meteor Trails" Proceedings of the IEEE, Vol 52, Feb. 1964, pp 116-136.

[16]. Villard, OG.; Eshleman, Von R.; Manninig, LA. and Peterson, AM. "The Role of Meteors In Extended-Range VHF Propagation" Proceedings of the IRE, Vol 43, Oct. 1955, pp 1473-1481.

[17]. Eshleman, Von R. "The Theoretical Length Distribution of Ionized Meteor Trails" Journal of Atmospheric and Terrestrial Physics, Vol 10, Pergamton Press Ltd. London, 1957, pp 57-72.

[18]. Manning, LA. and Eshleman, Von R. "Meteors In The Ionosphere" Proceedings of the IRE, Vol 47, Feb. 1959, pp 186-199.

[19]. Felber, F.; Davis, H.; Stahl, R. and Wright, D. "Concepts for Near Continuous Reception of VHF (Very High Frequency) Signals Using Meteor Burst Propagation" JAYCOR, San Diego, CA, Report No JAYCOR-J200-85-875/2393, July 1985.

[20]. Esleman, Von R. and Mlodnosky, RF. "Directional Characteristics of Meteor Propagation Derived from Radar Measurements" Proceedings of the IRE, Vol 45, Dec. 1957, pp 1715-1723.

[21]. Gray, KG. "Meteor Burst Communications" Signal (USA), Vol 36, No 9, May 1982, pp 125-134.

[22]. Spezio, AE. "Meteor-Burst Communication Systems: Analysis and Synthesis" Naval Research Laboratory Report 8286, Washington, D.C., USA., Dec. 1978.

[23]. Helweg, QG. "Meteor-Burst Communications: Is This What the Navy Needs?" Naval Postgraduate Schoole, Monterey, CA., USA., Master dissertation, June 1987.

[24]. Weiss, AA. "The Incidence of Meteor Particles Upon the Earth" Australian Journal of Physics, Vol 10, pp 397-411.

[25]. Brown, DW. "A Physical Meteor-Burst Propagation Model and Some Significat Results for Communication System Design" IEEE Journal on Selected Area in Communications, Vol SAC-3, No 5, Sept. 1985, pp 745-755.

[26]. Eshleman, Von R. and Manning, LA. "Radio Communication by Scattering from Meteoric Ionization" Proceedings of the IRE, Vol 42, March 1954, pp 530-536.

[27]. Ince, AN. "Spatial Properties of Meteor Burst Propagation" IEEE Transaction on Communications, Vol COM-28, No 6, June 1980, pp 841-849.

[28]. Hines, CO. and Pugh, RE. "The Spatial Distribution of Signal Sources in Meteoric Forward-Scattering" Canadian Journal of Physics, Vol 34, Oct. 1956, pp 1005-1015.

[29]. Forsyth, PA.; Vogan, EL.; Hansen, DR. and Hines, CO. "The Principles of JANET-A Meteor-Burst Communication System" Proceedings of the IRE, Vol 45, Dec. 1957, pp 1642-1657.

[30]. Brown, DW. and Williams, HP. "The Performance of Meteor-Burst Communications at Different Frequencies" AGARD Conference Proceedings, Aspects of Electromagnetic Wave Scattering in Radio Communications, Cambridge Mass, Oct. 3-7, 1977, pp 24.1-24.6.

[31]. M[c]kinley, DWR. "Meteor Science and Engineering" M[c]graw-Hill Book Co., Inc., New York, 1961.

[32]. James, JC. and Meeks, NL. "On the Relative Contributions of Various Sky Regions to Meteor-Trail Communications" Georgia Institute of Technology, Atlanta, Georgia, Engineering Experiment Station, Technical Report No 1, Naval Research Contract No Nonr-991(02), June 1956, pp 1-65.

[33]. Eshleman, Von R. "Meteor Scatter" in "The Radio Noise Spectrum" Harvard University Press, Cambridge Mass, Ch. 4, 1960.

[34]. Steffancin, W. and Brown, D. "CSC (Computer Sciences Corporation) Meteor Burst Model Enhancement Test Report" Computer Sciences Corp., Fall Church, VA., Contract No DC100-84-C-0030. Feb. 1986.

[35]. Greenhow, JS. and Neufeld, EL. "Turbulance At Altitudes of 80-110 km and its Effects on Long-Duration Meteor Echoes" J Atmos. Terr. Phys., Vol 16, 1959, pp 384-392.

[36]. Kaiser, TR. "Radio Echo Studies of Meteor Ionization" Advances in Physics, Vol 2, 1953, pp 495-544.

[37]. Meeks, ML. and James, JC. "On the Influence of Meteor-Radiant Distributions in Meteor-Scatter Communication" Proc. of the IRE, Vol 45, Dec. 1957, pp 1724-1733.

[38]. Pugh, RE. "The Number Density of Meteor Trails Observable by the Forward-Scattering of Radio Waves" Can. J. Phys. Vol 34, April 1956, pp.997-1004.

[39]. Rudie, NH. "The Relative Distribution of Observable Meteor Trails in Forward Scatter Meteor Communications" Ph.D thesis, Mont. State Univ., Bozeman. 1967.

[40]. Weitzen, JA. "Predicting the Arrival of Meteors Useful for Meteor Burst Communication" Radio Science (USA), Vol 21, No. 6, Nov. 1986, pp 1009-1020.

[41]. Davies, JG. "Radio Observations of Meteors" Advancees in Electronics and Electron Physics, Vol 9, Academic, Orlando, Fla., 1957, pp 95-128.

[42]. Lord Rayleigh, "The Theory of Sound" The Macmillan Company, NY., USA., Vol. 1 (1877,1937), pp. 98 and 150-157, and Vol. 2 (1878,1929), p. 145.

[43]. Carson, JR. "A Generalization of the Reciprocal Theorem" Bell System Tech. J., 3, July 1924, pp. 393-399.

[44]. Hansen, RC. "Fundumental Limitations in Antennas" Proceedings of the IEEE, Vol 69, No 2, Feb. 1981, pp 170-182.

[45]. Kraus, JD. "Antennas" McGraw-Hill Inc., Second Edition, 1988.

[46]. Roy, TN. "Airborne Man-Made Radio Noise Assessment" Naval Ocean Systems Center (NOSC) San Diego, USA, April 1981.

[47]. Rudge, AW.; Milne, K.; Olver, AD. and Knight, P. "The Handbook of Antenna Design" Vol 1, Peter Peregrinus Ltd., London, UK, 1982.

[48]. Williams, HP. "Antenna Theory and Design" Vol 2, Sir Isaac Pitman & Sons Ltd., London 1966, pp 318-329.

[49]. Spaulding, AD. and Disney, RT. "Man-Made Radio Noise, Part I, Estimates for Business, Residential and Rural Areas" US Dept. of Commerce, OT Report 74-38, June 1974.

[50] Bodman, GHW. Personal Communication; The South African Value Management Foundation; P O Box 1894, Rivonia, Sandton 2128, RSA.

[51] Handley, P. Personal Communication; SALBU(PTY)Ltd.; P O Box 109, Irene 1675, RSA.

[52]. Givati, O.; Clark, AR. and Fourie, APC. "Intelligent Pre-Processor for NEC Antenna Design Software" 5th Annual Review of Progress in Applied Computational Electromagnetics, Conf. Proc., March 1989, pp.572-583.

[53]. Kraus, JD. "Electromagnetics" McGraw-Hill Inc., Third Edition, 1984.

[54]. Nes, H. "Meteor Burst Polarization Trails" Elec. Letters (GB), Vol. 21, No. 24, Oct.1985, pp. 1132-1133.

[55] Altshuler, EE. "The Travelling-Wave Linear Antenna" IRE Trans. on Antennas and Propagation, Vol. AP-9, No. 4. 1961.

[56]. Thiele, GA. "Wire Antennas" Chapter 2 in "Computer Techniques for Electromagnetics" By Mittra, R., Pergamon Press, 1973, pp 7-73.

[57]. Hansen, PM. "The Radiation Efficiency of Dipole Antenna Located Above an Imperfect Conducting Ground" IEEE Trans. in Antennas and Propagation, Vol AP-20, No. 6, Nov. 1972, pp 766-770.

[58]. Austin, BA. and Fourie, APC. "Numerical Modelling and Design of Loaded Broadband Wire Antennas" IEE Fourth International Conference on HF Radio Systems and Techniques, April 1988, pp 125-129.

[59]. Kubina, SJ. "Numerical Modelling Methods for Predicting Antenna Performance on Aircraft" AGARD Lecture Series No. 131, Sept. 1983, pp 9-1 to 9-38.